Міністерство освіти і науки України
Харківський національний університет імені В. Н. Каразіна

Факультет (навчально-науковий інститут) «Фізико-технічний факультет»

Кафедра Фізики ядра та високих енергій імені О. І. Ахієзера

До захисту допущено
Кафедрою Фізики ядра та високих енергій імені О. І. Ахієзера протокол № 10 від 15.05.2026 р.

завідувач кафедри _____ Юрій Слюсаренко
(підпис) *(ім'я, прізвище)*

«15» травня 2026 р.

Кваліфікаційна робота
здобувача другого (магістерського) рівня вищої освіти
(першого (бакалаврського) / другого (магістерського))

Швидкі неадіабатичні нерезонансні квантові логічні вентилі в дисипативному середовищі
(назва роботи)

Спеціальність (спеціалізація) 105 «Прикладна фізика та наноматеріали»
(код та найменування спеціальності; спеціалізації спеціальності - за наявності)

Освітня програма "Експериментальна ядерна фізика та фізика плазми"
(назва освітньої програми)

Виконавець _____ Богдан Кушнарьов
(підпис) *(ім'я, прізвище)*

Науковий керівник _____ Сергій Шевченко
(підпис) *(ім'я, прізвище)*

Науковий керівник _____ Андрій Гах
(підпис) *(ім'я, прізвище)*

Харків – 2026

АНОТАЦІЯ

Мета роботи – аналіз переваг та недоліків, а також порівняння точності виконання квантових логічних вентилів на базі осциляцій Рабі та неадіабатичних переходів Ландау-Зінера-Штукельберга-Майорани (ЛЗШМ) у відкритих квантових системах.

Об'єкт дослідження – динаміка відкритих дворівневих квантових систем. **Предмет дослідження** – вплив процесів енергетичної релаксації та дефазування на точність виконання однокубітного X-вентиля за допомогою осциляцій Рабі та ЛЗШМ переходів.

Результати й наукова новизна – шляхом чисельного інтегрування рівнянь Блоха отримано просторові розподіли точності на сфері Блоха залежно від початкового стану кубіта для X-вентиля та виявлено супутні патерни похибок. Кількісно доведено перевагу ЛЗШМ-переходів як більш стійких до дисипативних процесів порівняно з резонансними методами контролю.

Висновки – резонансні методи керування (з використанням осциляцій Рабі) є критично вразливими до дефазування через велику тривалість виконання логічних вентилів. Тим часом неадіабатичні ЛЗШМ-переходи забезпечують високу швидкість обчислень, мінімізуючи час взаємодії кубіта з навколишнім середовищем.

Ключові слова: кубіт, матриця густини, рівняння фон Неймана, діабатичний базис, адіабатичний базис, осциляції Рабі, рівняння Блоха, час релаксації, час декогеренції, квазіперетин, переходи Ландау-Зінера-Штукельберга-Майорани, метод переносних матриць, точність.

ABSTRACT

Objective of the study – analysis of the advantages and disadvantages, as well as comparison of the fidelity of quantum logic gates based on Rabi oscillations and non-adiabatic Landau-Zener-Stückelberg-Majorana (LZSM) transitions in open quantum systems.

Object of research – dynamics of open two-level quantum systems. **Subject of research** – the influence of energy relaxation and dephasing processes on the fidelity of a single-qubit X-gate executed using Rabi oscillations and LZSM transitions.

Results and scientific novelty – by numerically integrating the Bloch equations, spatial distributions of fidelity on the Bloch sphere depending on the initial state of the qubit for the X-gate were obtained, and concurrent error patterns were identified. The advantage of LZSM transitions as being more robust to dissipative processes compared to resonant control methods has been quantitatively proven.

Conclusions – resonant control methods (using Rabi oscillations) are critically vulnerable to dephasing due to the long execution time of the logic gates. Meanwhile, non-adiabatic LZSM transitions provide high computational speed, minimizing the interaction time of the qubit with the environment.

Keywords: qubit, density matrix, von Neumann equation, diabatic basis, adiabatic basis, Rabi oscillations, Bloch equations, relaxation time, decoherence time, avoided crossing, Landau-Zener-Stückelberg-Majorana transitions, transfer-matrix method, fidelity.

Contents

INTRODUCTION

The development of scalable quantum computing systems is one of the most important challenges in modern physics and engineering. A key obstacle to the practical implementation of quantum algorithms is the interaction of quantum systems (qubits) with the surrounding dissipative environment. This interaction leads to energy relaxation and dephasing processes that irreversibly destroy quantum coherence. In the modern era of noisy intermediate-scale quantum devices (NISQ), when full quantum error correction is not yet available, it is critical to create control protocols that are as robust to interference as possible. Traditional resonant control methods based on Rabi oscillations have fundamental speed limitations because they require weak control fields, which makes them vulnerable to dissipation. In this regard, the study of alternative, ultrafast non-adiabatic control methods, in particular based on Landau–Zinner–Stückelberg–Majorana (LZSM) transitions, is an extremely urgent task for the optimization of quantum logic gates.

The work is the first to directly quantitatively compare spatial fidelity distributions for resonant and non-adiabatic control methods outside the rotating wave approximation (RWA). Specific topological error patterns are identified and physically substantiated.

SECTION 1. LITERATURE REVIEW

This section presents information from modern scientific works and articles concerning quantum gates based on Rabi oscillations and non-resonant Landau-Zener transitions. Special attention is paid to recent research regarding methods for optimizing computations based on them, as well as comparing the results of both gate implementation methods.

1.1 Historical perspective on quantum computing

Since the early stages of quantum mechanics' formation as a separate science, various ideas arose for using its unique mathematical apparatus to perform ultrafast and precise computations. In the 1930s, this initiated the search for methods to create conceptually new computing machines that would rely on the quantum properties of the world. However, despite enormous prospects, the problem of creating an analog to a modern computer that would operate on the basis of quantum physics laws is currently unsolved due to numerous theoretical and experimental problems. In particular, one of the key issues is the selection of the optimal variant of the physical quantum system with which computations would be performed, and the direct methods for controlling the states of this system.

Many different ways of physical realization of qubits (the simplest quantum systems) have now been proposed. Among them are ion traps, superconducting qubits, semiconductor qubits (spin-based), topological and photonic qubits, etc. [1–3]. However, historically, one of the simplest and most common variants originated outside of quantum mechanics altogether.

In 1922, the Stern-Gerlach experiment proved the existence of spin as a physical quantity [4]. By applying a magnetic field to particles, it was possible to separate them into two beams according to the direction of the spin projection. But the exact value of the magnetic moment of the nucleus was impossible to obtain due to the spatial blurring of these beams during the experiment. Later, in 1937, the outstanding physicist Isidor Isaac Rabi found a solution to this problem [5]. He proposed adding a weak oscillating magnetic field component to a strong constant one. The idea was that if the frequency of the external alternating field exactly matched the Larmor frequency (i.e., the frequency of spin precession) [6], the particles would begin to resonate, manifesting in energy absorption and a change in spin orientation. In 1938, this was proven experimentally [7], and in 1944, Rabi

received the Nobel Prize for his discovery. The proposed method not only allowed for the measurement of nuclear magnetic moments but also found practical application in many other inventions. It underlies the operation of atomic clocks and medical tomography. Over time, this idea became one of the most common variants for the resonant control of spin-based qubits [3].

Within the scope of this work, an alternative control paradigm based on the theory of non-resonant non-adiabatic transitions is also considered. Although its concept was proposed even earlier than the discovery of Rabi oscillations, it did not gain widespread use at the time. The foundation of this theory was formed in 1932 in four independent works [8, 9]. Their authors (Lev Landau, Clarence Zener, Ernst Stückelberg, and Ettore Majorana) investigated the behavior of quantum systems in the vicinity of an avoided-level crossing [10–13]. Each of them made a unique contribution to the study of the effect now known as Landau-Zener-Stückelberg-Majorana (LZSM) transitions. In particular:

– Landau investigated the system's behavior in the quasi-adiabatic limit and developed an approach that allows correctly describing transitions between energy levels where they approach each other;

– Zener also analyzed the asymptotic behavior of the system and derived an exact analytical formula for the transition probability of a two-level qubit whose parameters depend linearly on time;

– Stückelberg drew attention to the accumulation of a relative phase between non-adiabatic transitions and showed that the probability amplitudes during two consecutive passages interfere with each other;

– Majorana described non-adiabatic transitions for multi-level systems with arbitrary spin in an alternating magnetic field, essentially generalizing the results.

For a long time, the proposed theory was used primarily in atomic and molecular physics. However, with the emergence of the ability to create macroscopic quantum systems (for example, superconducting qubits), LZSM interferometry has become one of the main tools for their control [8, 14].

1.2 Problems due to the influence of a dissipative environment

Another reason why the question of choosing optimal methods for the realization and control of quantum systems arises at all is the impossibility of creating ideal isolation

for it from the environment. The interaction of the system with the environment leads to the loss of internal information and, as a result, to a significant decrease in the accuracy of the results. Besides the obvious need to find ways to improve isolation, this imposes limitations on the allowable execution time of computations. That is, the creation of scalable quantum processors also requires an increase in gate speed to perform as many operations as possible within the system's coherence time. This raises the question of the accuracy or even the applicability of modern control methods.

Despite the simplicity and convenience of implementation, controlling the state of qubits using Rabi oscillations has a number of fundamental and technological limitations. In particular, they concern attempts to increase the execution speed of operations by this method. In practice, this is achieved by increasing the amplitude of the driving magnetic field, which entails a lot of problems. First, it leads to the violation of the Rotating-Wave Approximation (RWA), which is applicable only for weak fields [15]. Fast harmonics begin to strongly distort the shape of probability oscillations, which cease to be harmonic. Second, the problem of leakage arises to energy levels outside the computational subspace, leading to the loss of information about the system's state [16]. However, reducing the field amplitude and the speed of gate execution does not make the result ultra-precise either, because another problem arises. The interaction of the system with a dissipative environment leads to dephasing and relaxation processes, which destroy quantum superposition. And if the characteristic execution time of a Rabi gate becomes on the same order of magnitude as the system's decoherence time, the fidelity of the logical gate drops rapidly (exponentially) even before completing at least one slow resonant gate. This creates a need to develop alternative fast and precise control methods.

The use of LZSM transitions allows getting rid of many of the mentioned limitations. Unlike Rabi oscillations, LZSM gates are executed using non-resonant high-amplitude pulses and require significantly less exposure time to an external field. This provides a substantially higher execution speed of operations, which is a critical factor in minimizing the dissipative influence of the environment. In addition, studies show that the LZSM transition method also provides higher robustness [17], the ability to use baseband pulses [16], eliminating the need for complex microwave control signals, and also reduces the impact of environmental noise on the quantum computing process [18].

However, although LZSM transitions eliminate a significant part of the problems present in the resonant Rabi method, this does not indicate a complete absence of drawbacks. In particular, the accuracy of this method strongly depends on the duration and shape of the driving pulses [19, 20], and its application to multi-qubit systems is a significantly more complex engineering task [19]. Moreover, it has been established that a single LZSM transition often cannot provide a 100% probability of state change with sufficient accuracy [19].

1.3 Modern methods for improving the accuracy of quantum computing

The current stage of quantum computing technology development is often defined as the era of Noisy Intermediate-Scale Quantum (NISQ) devices. The creation of full-scale quantum computers is currently problematic due to the unresolved issue of isolating qubits from a dissipative environment or reducing its impact. Therefore, research is currently moving in two different, though similar in goal, directions. Besides choosing a more promising method (physical concept) for the implementation of quantum gates, reducing computation errors can be achieved both through various algorithmic methods of Quantum Error Correction (QEC) and directly through hardware optimization of the chosen control method (Optimal Control Theory, OCT).

For example, the simplest way to improve the accuracy of gates based on Rabi oscillations is the application of Gaussian pulse envelopes. This allows minimizing adiabatic losses and reducing spectral broadening [2, 21]. For operations based on LZSM, a larger even number (2, 4, or even more) of transitions is often used to execute a single logical gate. Despite the increase in the time of a single operation, this allows reducing computation errors [19]. An even more interesting and important fact is that even unoptimized LZSM-based gates provide higher accuracy than optimized Rabi-based ones (see Fig. 1.1).

There are also more complex methods for optimization and searching for optimal driving field profiles even in the presence of a dissipative environment influence. Among them:

– Gradient Ascent Pulse Engineering (GRAPE). It consists of breaking down a complex control signal into a series of short ones, each having a constant amplitude. This is accompanied by an iterative calculation of the fidelity function's gradient with respect to the characteristics of each segment, followed by adjustment [23];

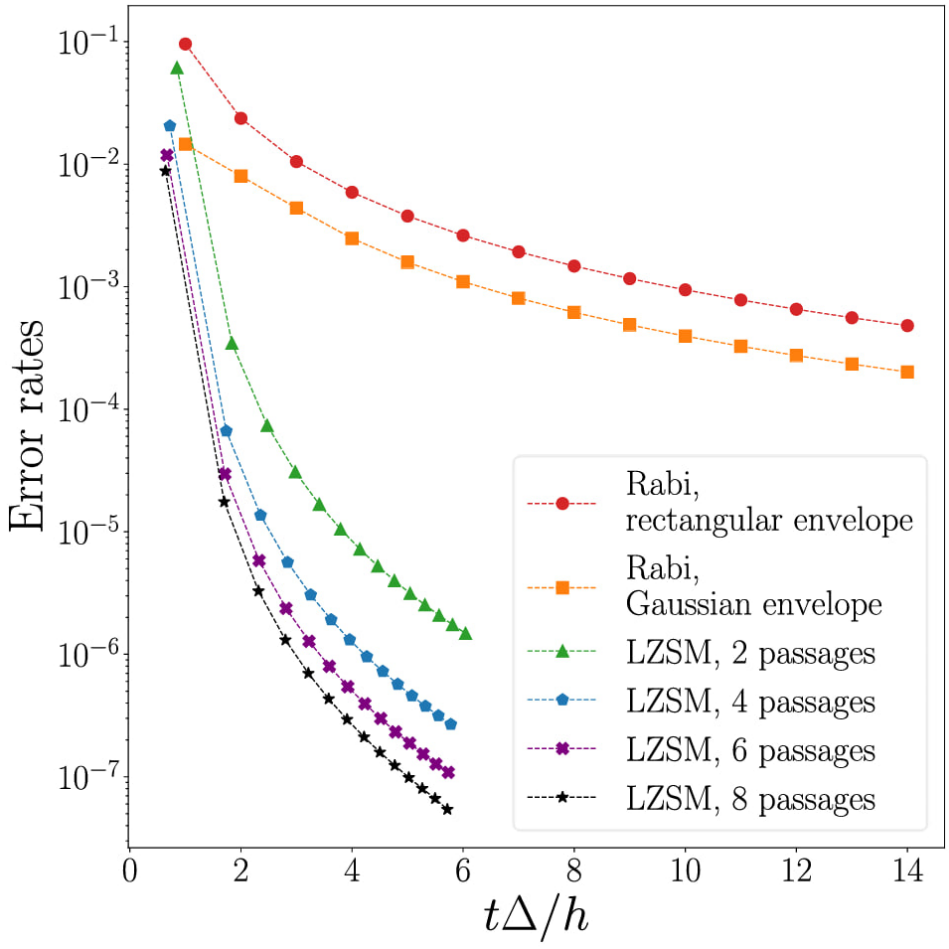

Figure 1.1 – Comparison of error rates for Rabi and LZSM approaches for the realization of single-qubit Y-gate [19]. Δ here denotes tunneling amplitude. The error rates for both approaches calculated for different gate durations $\frac{t\Delta}{h}$. For the Rabi implementation, the gate duration equals an integer number of periods of a resonant driving (from 1 to 14). Increasing the gate duration, the error for the LZSM approach decreases much faster than for the Rabi approach.

– Krotov's method. Unlike GRAPE, this method works with continuous control fields. It is also an iterative algorithm that guarantees a monotonic increase in gate fidelity at each step. It is highly effective for optimizing the evolution of multidimensional open quantum Markov systems (i.e., those whose dynamics are described by the Lindblad equation or similar to it) [21,22].Regarding methods of Quantum Error Correction (QEC), overcoming the noise problem in a global perspective is possible through the transition

to Fault-Tolerant Quantum Computing (FTQC). The algorithms used in this process (e.g., Surface Codes) encode the information of one logical qubit in the entangled state of an ensemble of many physical realizations of this same qubit, allowing for error checking without directly measuring the state [24].

However, the application of QEC requires overcoming the so-called fault-tolerance threshold: the physical error of each individual gate must not exceed a certain critical level (usually $\sim 10^{-2} - 10^{-3}$). Therefore, even for the practical applicability of such error correction algorithms, research into physical dissipation mechanisms and the search for alternative quantum control methods are necessary. In particular, non-adiabatic LZSM transitions are highly promising in this context, as they provide high speed and accuracy of computations, which is critically important for QEC. Reducing gate errors at the hardware level directly enables the practical implementation of large-scale quantum error correction methods, further increasing the overall accuracy of quantum computing.

SECTION 2. BASIC INFORMATION ABOUT QUANTUM SYSTEMS

This section presents the basic terms and formulas necessary for a fundamental understanding of quantum mechanics and, in particular, the theory of quantum computing. The simplest quantum circuits are considered using the theoretical foundations of quantum computing theory and various methods of their physical implementation.

2.1 Uncertainty of quantum systems

Any particle is quantum by its nature and has properties different from those of classical bodies. To demonstrate this, let us consider a monochromatic wave with energy ϵ and frequency ω. From the perspective of wave-particle duality, it depends on the number of photons N and is proportional to the square of the electric field amplitude E:

$$\epsilon = N\hbar\omega \sim E^2, \tag{2.1}$$

where $\hbar$ is the reduced Planck constant.

Let this wave fall on a system of a polarizer and an analyzer, which are located at an angle θ to each other. After passing through the polarizer, the energy and amplitude of the wave intensity will become ϵ_0 and E_0 respectively, and after the analyzer – ϵ_{past} and E_{past}. The transmitted and blocked components ϵ_{block}, E_{block} can be written as

$$E_{past} = E_0 \cos\theta, \quad E_{block} = E_0 \sin\theta, \tag{2.2}$$

$$\epsilon_{past} = \epsilon_0 \cos^2\theta, \quad \epsilon_{block} = \epsilon_0 \sin^2\theta. \tag{2.3}$$

Similar expressions for the number of transmitted N_{past}, blocked N_{block}, and photons before the analyzer N_0 follow from (2.1) and (2.3):

$$N_{past} = N_0 \cos^2\theta, \quad N_{block} = N_0 \sin^2\theta. \tag{2.4}$$

Let us now consider the case $N_0 = 1$. The expression (2.4) will change to

$$N_{past} = \cos^2\theta \leq 1, \quad N_{block} = \sin^2\theta \leq 1. \tag{2.5}$$

At the same time, it becomes obvious that N_{past}, N_{block} must be less than 1, which is fundamentally impossible for the number of photons as such. Then they should denote not the number of transmitted and blocked photons, but the probabilities of transmission P_{past} and blocking P_{block}. As we can see, the total probability P is equal to 1 and is completely correctly defined as

$$P_{past} = \cos^2\theta,\ P_{block} = \sin^2\theta \to P = P_{past} + P_{block} = \cos^2\theta + \sin^2\theta = 1. \quad (2.6)$$

Thus, in this example, one can verify that quantum systems fundamentally have a statistical and probabilistic character [25].

2.2 Methods of defining a qubit state

Let us now consider various options for describing the state of a single-particle quantum system.

2.2.1 Wave function. Bloch vector and sphere

In quantum information theory, the unit of information measurement is the quantum bit (qubit). Unlike a classical bit – which takes only the value 0 or 1 – mathematically, a qubit is described by a wave function $|\psi\rangle$, which is a vector in a two-dimensional Hilbert space, defined as a linear superposition of two mutually exclusive states $|0\rangle$ and $|1\rangle$:

$$|\psi\rangle = a\,|0\rangle + b\,|1\rangle = a\begin{pmatrix}1\\0\end{pmatrix} + b\begin{pmatrix}0\\1\end{pmatrix} = \begin{pmatrix}a\\b\end{pmatrix}, \quad (2.7)$$

where a, b are the complex probability amplitudes of finding the system in these states, respectively.

By definition, a, b must satisfy the normalization condition

$$|a|^2 + |b|^2 = 1. \quad (2.8)$$

The states represent completely mutually exclusive outcomes, so they must also be orthonormal:

$$\langle n|m\rangle = \delta_{nm}, \quad n, m = 0, 1, \quad (2.9)$$

where δ_{nm} is the Kronecker delta.

Taking into account condition (2.8), as well as the postulate of quantum mechanics that $|\psi\rangle$ and $c\,|\psi\rangle$ correspond to the same state (here c is some purely complex multiplier), we obtain that a, b are described by only two independent real parameters. The simplest way to express them through the angles of a spherical coordinate system θ, ϕ is as

$$a = \cos\frac{\theta}{2}, \quad b = e^{i\phi}\sin\frac{\theta}{2}, \tag{2.10}$$

moreover, the division by 2 in the arguments arises as a consequence of condition (2.9).

Thus, a qubit state can be specified not only by the wave function (2.7), but as a certain point on a sphere with a unit radius. Its coordinates can be given as

$$\vec{R} = (\sin\theta\cos\phi, \sin\theta\sin\phi, \cos\theta). \tag{2.11}$$

The resulting vector $\vec{R}$ is called the Bloch vector, and the sphere of qubit states is called the Bloch sphere [26] (Fig. 2.1).

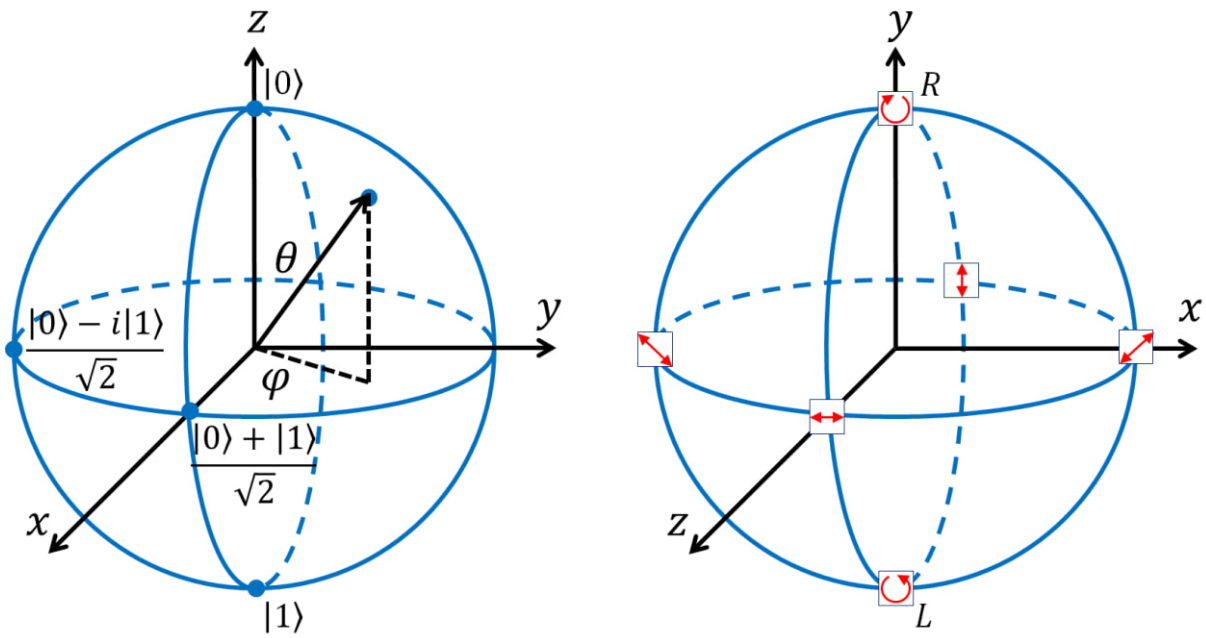

Figure 2.1 – Bloch sphere (left panel) and Poincaré sphere (right panel) are identical up to a rotation

Note that a qubit is not a purely mathematical abstraction. Physically, it can be any quantum system that exists with certain probabilities in two different pure states. In particular, in 2.1 it was shown that a photon can be used as a physical implementation of a qubit. Then its pure states are considered to be plane polarizations $|e_x\rangle$, $|e_y\rangle$ in the x and y planes, and an arbitrary state $|e\rangle$ is their superposition:

$$|e\rangle = \cos\frac{\theta}{2}|e_x\rangle + e^{i\phi}\sin\frac{\theta}{2}|e_y\rangle. \tag{2.12}$$

Physically, an arbitrary state $|e\rangle$ corresponds to a certain elliptical polarization, which makes the Poincaré sphere (see Fig. 2.1) an equivalent to the Bloch sphere for photonic qubits [26, 27].

2.2.2 Mixed states. Density matrix

However, in practice, it turns out that a qubit state cannot always be correctly described as a point on the Bloch sphere. The reason for this is the interaction of the qubit with the environment. Considering that no quantum system can be completely isolated, and knowing the exact state of the environment (essentially, the whole world) is simply impossible, information about the system's state is lost as a result of their interaction. The qubit transitions from a pure state $|\psi\rangle$ to a so-called mixed state, where there are several possible states of the system (a statistical ensemble), which are described by certain wave functions $|\psi_i\rangle$. Each of them is physically realized with a probability p_i, and as expected, the condition $\sum_i p_i = 1$ is fulfilled.

Therefore, it is necessary to find a way to correctly describe systems in mixed states. Physically, these states correspond to points inside the Bloch sphere, so the Bloch vector by definition (2.11) is not suitable. This problem can be solved using a special operator called the density matrix ρ (here and below, operators will be written without circumflexes):

$$\rho = \sum_i p_i |\psi_i\rangle\langle\psi_i|. \tag{2.13}$$

Obviously, pure states can also be described using ρ. For them, it expectedly follows that

$$p_1 = 1 \to \rho = \sum_{i=1}^{1} p_i \, |\psi_i\rangle \langle\psi_i| = |\psi\rangle \langle\psi| \, . \tag{2.14}$$

The main properties of the density matrix, in particular its Hermiticity and its trace being equal to 1, follow from the newly obtained expression:

$$\rho^\dagger = \rho, \tag{2.15}$$

$$\mathrm{Tr}(\rho) = 1. \tag{2.16}$$

Now let us find the values of the elements of the density operator ρ_{nm}. To do this, consider some basis $\{|e_k\rangle\}$, in which the wave functions are defined as

$$|\psi_i\rangle = \sum_k a_k^{(i)} \, |e_k\rangle \, , \tag{2.17}$$

where $a_k^{(i)}$ are the probability amplitudes of finding the system in the basis states $|e_k\rangle$ of the i-th component of the statistical mixture.

Then, using the orthonormality condition of the basis vectors $\langle e_i|e_j\rangle = \delta_{ij}$, we express the elements of the operator ρ as

$$\rho_{nm} = \langle e_n|\rho|e_m\rangle = \sum_i p_i \langle e_n|\psi_i\rangle\langle\psi_i|e_m\rangle =$$

$$= \sum_{i,j,k} p_i a_j^{(i)} a_k^{(i)*} \langle e_n|e_j\rangle\langle e_k|e_m\rangle = \sum_i p_i a_n^{(i)} a_m^{(i)*}. \tag{2.18}$$

Let us now analyze the physical meaning of the elements of the density matrix:

1) For diagonal elements $m = n$, then $\rho_{nn} = \sum_i p_i |a_n^{(i)}|^2$. By definition, p_i is the probability of realization of the quantum mechanical state $|\psi_i\rangle$, and from formula (2.18) it follows that $|a_n^{(i)}|^2$ is the probability of the system being in the basis state $|e_n\rangle$ of the i-th component of the statistical ensemble. Thus, ρ_{nn} determines the overall probability of finding the system in the state $|e_n\rangle$. Therefore, the diagonal elements of the density operator are called the populations of the corresponding states. Moreover, the expected

result holds true for them:

$$\sum_n \rho_{nn} = \sum_i p_i \sum_n |a_n^{(i)}|^2 = \sum_i p_i = 1. \quad (2.19)$$

2) Off-diagonal elements ρ_{nm} contain multipliers $a_n^{(i)} a_m^{(i)*}$, which simultaneously describe both states – $|e_n\rangle$ and $|e_m\rangle$. So physically, these elements characterize the interaction (interference) between the indicated states in the i-th component of the statistical ensemble. Therefore, the off-diagonal elements of the density operator are called coherences.

Thus, the density operator ρ unambiguously describes even the states of open quantum systems, so it can be used instead of wave functions $|\psi_i\rangle$.

2.3 Description of qubit state evolution

If a point on the Bloch sphere corresponds to the system state, then the movement along the sphere determines the qubit evolution (a transition inside the Bloch sphere indicates dissipative processes). In a general sense, there are two different options for exactly how to describe the system's evolution. Let's consider them separately.

2.3.1 Basic quantum gates

Let us first consider the evolution from the perspective of quantum information theory. If the system has n mutually exclusive states and is described by the vector (2.7), then multiplying it by an arbitrary $n \times n$ matrix will correspond to a transition to a new state. Note that unitary transformations U are characteristic of an isolated quantum system (they preserve state purity). This follows from formulas (2.8)-(2.9):

$$\langle\psi'|\psi'\rangle = \langle\psi|U^\dagger U|\psi\rangle = 1 \rightarrow U^\dagger U = I \rightarrow U^\dagger = U^{-1}, \quad (2.20)$$

where I is the identity matrix.

Unitary transformations of a system of one or more qubits are called quantum gates. In particular, the Pauli matrices can be considered as the simplest gates [26, 28]

$$\sigma_x = X = \begin{pmatrix} 0 & 1 \\ 1 & 0 \end{pmatrix}, \quad \sigma_y = Y = \begin{pmatrix} 0 & -i \\ i & 0 \end{pmatrix}, \quad \sigma_z = Z = \begin{pmatrix} 1 & 0 \\ 0 & -1 \end{pmatrix}. \tag{2.21}$$

It is easy to verify that the result of the action of these operators on an arbitrary qubit state are rotations of the Bloch vector by an angle π around the corresponding axis $\sigma_i = R_i(\pi)$, where $i = x,y,z$. In the general case, the rotation of the state vector around one of these axes by an arbitrary angle ϕ is given by the formula

$$R_{x,y,z}(\phi) = \exp\left(-i\sigma_{x,y,z}\frac{\phi}{2}\right) = \cos\left(\frac{\phi}{2}\right) - i\sin\left(\frac{\phi}{2}\right)\sigma_{x,y,z}. \tag{2.22}$$

Obviously, any unitary transformation can theoretically be defined as a sequential application of two rotations around the principal axes. For example, the Hadamard gate H [28] can be defined as

$$H = R_y(\pi/2)R_z(\pi) = \sqrt{YZ} = \frac{1}{\sqrt{2}}\begin{pmatrix} 1 & 1 \\ 1 & -1 \end{pmatrix}. \tag{2.23}$$

Another important consequence of the unitarity of quantum operations is that an arbitrary logic gate G is equivalent to itself with some complex multiplier of unit modulus:

$$G \leftrightarrow e^{i\varphi}G, \tag{2.24}$$

where φ is an arbitrary angle.

2.3.2 Liouville-von Neumann equation

Let us now consider the evolution of the system from the perspective of dynamics. The generator of the evolution operator is the Hamiltonian H (here and below, this symbol denotes exactly Hamiltonians, unless specified otherwise), and the direct change in the

qubit state over time t is described by the Schrödinger equation:

$$H(t)\,|\psi(t)\rangle = i\hbar\frac{d}{dt}\,|\psi(t)\rangle\,. \tag{2.25}$$

However, as was noted in 2.2.2, wave functions, unlike density matrices, describe only pure states, so it is necessary to obtain an equivalent of the Schrödinger equation for ρ. Thus, we will find the time derivative of (2.13) and substitute into the resulting expression similar derivatives of the wave functions from (2.25). This gives us a result that is called the Liouville-von Neumann equation (or simply von Neumann equation) in the scientific literature [29, 30]:

$$\dot{\rho} = \frac{d}{dt}\sum_i p_i\,|\psi_i\rangle\langle\psi_i| = \sum_i p_i\big(|\dot{\psi}_i\rangle\langle\psi_i| + |\psi_i\rangle\langle\dot{\psi}_i|\big) = \sum_i p_i\bigg(\frac{1}{i\hbar}H\,|\psi\rangle\langle\psi| -$$
$$-\,|\psi\rangle\langle\psi|\,H\frac{1}{i\hbar}\bigg) = -\frac{i}{\hbar}\sum_i p_i\big(H\,|\psi_i\rangle\langle\psi_i| - |\psi_i\rangle\langle\psi_i|\,H\big) = -\frac{i}{\hbar}[H,\rho]. \tag{2.26}$$

It is clear that the dynamics of a point's movement on the Bloch sphere are determined exactly by the Hamiltonian $H(t)$, which is formed as a result of intrinsic passive evolution H_0 and external driving influence on the qubit $V(t)$. However, it turns out that realizing arbitrary transitions experimentally is very difficult. As a result, not even a single one of the simplest gates mentioned in 2.3.1 can be executed as a sequence of exact rotations around specified axes. However, this fact itself is not a fundamental problem. Considering that gates define only the initial and final states of a qubit, the intermediate path can be chosen arbitrarily within the physical capabilities of the control mechanism. Therefore, one of the main tasks in the process of creating quantum computers is the search for effective methods of implementing arbitrary gates. In particular, one of the options will be analyzed in more detail in 4.2.

2.4 Basis states of a spin-based single-qubit system

Besides photons, another physical implementation of qubits is particles with spin $1/2$. Spin-based qubits will be considered exclusively hereafter. As the two mutually exclusive states (i.e., $|0\rangle$ and $|1\rangle$), one can choose states in which the spin projection value

on the z axis is $+1/2$ and $-1/2$, respectively. For a single-qubit system, they form a complete basis. Such a basis is called diabatic [8, 19].

Consider the Hamiltonian of a particle with spin [31, 32]. In the general case, it is expressed as

$$H_{full} = \frac{1}{2m}\left(\vec{p} - \frac{q}{c}\vec{A}\right)^2 + q\varphi - \vec{\mu}\vec{H}, \tag{2.27}$$

where m is the particle mass, $\vec{p}$ is its momentum operator, q is the charge, c is the speed of light, $\vec{A}$, φ are the vector and scalar potentials respectively, $\vec{\mu}$ is the magnetic moment operator, $\vec{H}$ is the magnetic field.

The first two terms in this expression account for the kinetic and potential energies of the particle in a magnetic field. Thus, we are only interested in the last term, the spin component $H = -\vec{\mu}\vec{H}$. In particular, for an electron, this term can be rewritten as

$$H = \frac{1}{2}g\mu_B\vec{\sigma}\vec{H}, \tag{2.28}$$

where g is the Landé factor (which is approximately equal to 2 for an electron), $\mu_B = \frac{|e|\hbar}{2mc}$ is the Bohr magneton, and $\vec{\sigma} = (\sigma_x, \sigma_y, \sigma_z)$.

Thus, the control of a spin qubit is carried out using a magnetic field. We will further consider the simplest case, namely $\vec{H} = (H_x, 0, H_z(t))$, where the constant component is necessary for splitting energy levels, and the variable one allows making spin transitions [6, 19]. Then the Hamiltonian of such a qubit can be written as

$$H = -\frac{\Delta}{2}\sigma_x - \frac{\varepsilon(t)}{2}\sigma_z, \tag{2.29}$$

where Δ is called the tunneling amplitude, and $\varepsilon(t)$ is the energy bias.

2.4.1 Transition to the adiabatic basis (via eigenvalue search)

Let us find the stationary energy levels of a spin qubit. Let the energy shift vary according to a harmonic law

$$\varepsilon(t) = \varepsilon_0 + A\cos\omega t, \tag{2.30}$$

where ε_0 is the offset, A is the amplitude, ω is the frequency of the magnetic field change.

As suggested in 2.3.2, let us separate the Hamiltonian into constant and variable components

$$H(t) = H_0 + V(t) \to H_0 = -\frac{\Delta}{2}\sigma_x - \frac{\varepsilon_0}{2}\sigma_z,\ V(t) = -\frac{A\cos\omega t}{2}\sigma_z. \tag{2.31}$$

Substituting formula (2.7) into (2.31), we will now solve the stationary Schrödinger equation

$$H_0\,|\psi\rangle = E\,|\psi\rangle \to (H_0 - E)\,|\psi\rangle = -\frac{1}{2}\begin{pmatrix} \varepsilon_0 + 2E & \Delta \\ \Delta & -\varepsilon_0 + 2E \end{pmatrix}\begin{pmatrix} a \\ b \end{pmatrix} = 0. \tag{2.32}$$

Using linear algebra tools, we find the eigenvalues and eigenfunctions of the operator H_0 by equating the determinant of the resulting matrix to zero

$$\begin{vmatrix} \varepsilon_0 + 2E & \Delta \\ \Delta & -\varepsilon_0 + 2E \end{vmatrix} = 0 \to 4E^2 - \varepsilon_0^2 - \Delta^2 = 0 \to$$

$$\to E = E_\pm \equiv \pm\frac{1}{2}\sqrt{\Delta^2 + \varepsilon_0^2} \equiv \pm\frac{1}{2}\Delta E, \tag{2.33}$$

where the quantity

$$\Delta E = E_+ - E_- = \sqrt{\Delta^2 + \varepsilon_0^2} \tag{2.34}$$

determines the distance between the stationary energy levels E_+ and E_-.

We continue to solve system (2.32). We express a through b from here and substitute it into the normalization condition (2.8). This gives the following results

$$a = -\frac{\Delta}{\varepsilon_0 + 2E}b \to b_\pm^2 = 1 - a^2 = \frac{1}{2}\left(1 \pm \frac{\varepsilon_0}{\Delta E}\right) \equiv \gamma_\pm^2, \tag{2.35}$$

$$a_\pm^2 = \frac{1}{2}\left(1 \mp \frac{\varepsilon_0}{\Delta E}\right) \equiv \gamma_\mp^2. \tag{2.36}$$

We get rid of the squares of a and b. To do this, we take into account the sign dependence between them

$$\operatorname{sgn} a = \mp \operatorname{sgn} b \to a_\pm = \gamma_\mp,\ b_\pm = \mp\gamma_\pm. \tag{2.37}$$

So, now we can move to the new (eigen) basis of the Hamiltonian

$$|E_-\rangle = \gamma_+ |0\rangle + \gamma_- |1\rangle, \tag{2.38}$$

$$|E_+\rangle = \gamma_- |0\rangle - \gamma_+ |1\rangle, \tag{2.39}$$

where

$$\gamma_\pm = \frac{1}{\sqrt{2}}\sqrt{1 \pm \frac{\varepsilon_0}{\Delta E}}. \tag{2.40}$$

The resulting basis $\{|E_+\rangle, |E_-\rangle\}$ is called adiabatic. Unlike the diabatic one $\{|1\rangle, |0\rangle\}$, in this basis, being in one of the eigenstates essentially means parallel $|E_+\rangle$ or anti-parallel $|E_-\rangle$ alignment of the particle's spin projection to the direction of the instantaneous magnetic field. The corresponding energy levels of both bases are depicted in Fig. 2.2. Note separately that in the case of $\Delta = 0$, both bases merge into one ($|E_-\rangle = |0\rangle$, $|E_+\rangle = |1\rangle$).

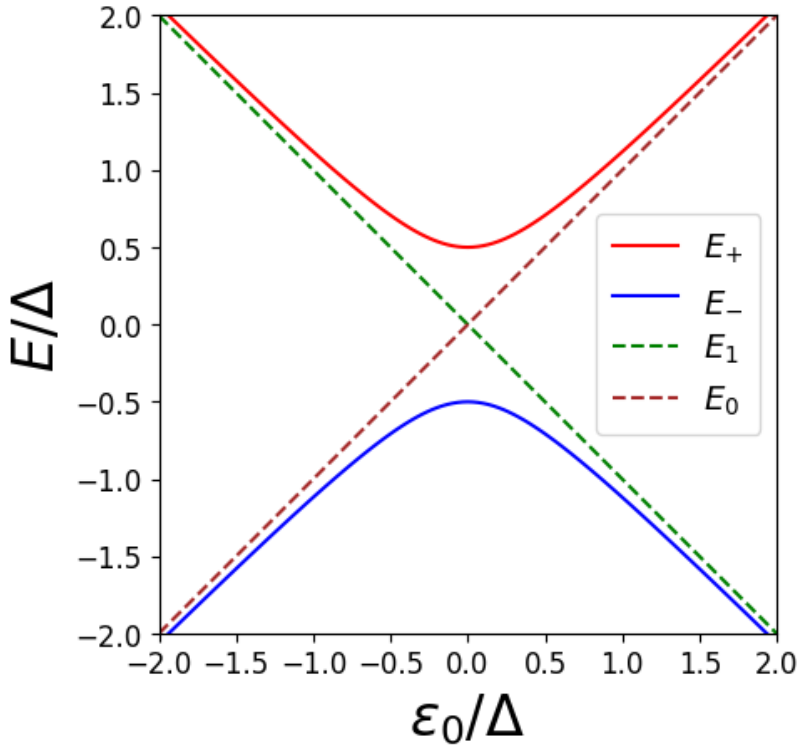

Figure 2.2 – Qubit energy levels in adiabatic $\{|E_+\rangle, |E_-\rangle\}$ and diabatic $\{|1\rangle, |0\rangle\}$ bases with dependence on the energy bias ε_0

2.4.2 Transition to the adiabatic basis (via rotation matrices)

Let us now consider another way to transition to the adiabatic basis. Obviously, the process of transitioning between two bases can always be considered as a rotation by some angle. In particular, the Hamiltonian from formula (2.29) is determined by a constant magnetic field lying in the xz plane. Let's make a rotation by some angle $\zeta \geq 0$ around the y axis so that the field is directed only along the z axis. Similar to formula (2.22), this transition will correspond to the rotation matrix

$$S = \exp\left(-\frac{i\zeta\sigma_y}{2}\right) = \cos\frac{\zeta}{2} - i\sin\frac{\zeta}{2}\sigma_y = \begin{pmatrix} \cos\frac{\zeta}{2} & -\sin\frac{\zeta}{2} \\ \sin\frac{\zeta}{2} & \cos\frac{\zeta}{2} \end{pmatrix}. \tag{2.41}$$

In the new basis, the wave function will be given as $|\psi'\rangle = S^{-1}|\psi\rangle$. Then from the Schrödinger equation, we find the new stationary Hamiltonian H_0'

$$|\psi\rangle = S|\psi'\rangle \to i\hbar S\frac{\partial}{\partial t}|\psi'\rangle = H_0 S|\psi'\rangle \to$$
$$\to i\hbar\frac{\partial}{\partial t}|\psi'\rangle = S^{-1}H_0 S|\psi'\rangle = H_0'|\psi'\rangle \to H_0' = S^{-1}H_0 S. \tag{2.42}$$

Since after such a rotation the magnetic field will be directed along the z axis, this will mean that H_0' has become completely diagonal. Then it can also be represented in the form

$$H_0' = -\frac{\Delta E}{2}\sigma_z \equiv -\frac{\Delta E}{2}(|E_-\rangle\langle E_-| - |E_+\rangle\langle E_+|). \tag{2.43}$$

We make a substitution from formula (2.41) into (2.42) and compare it with expression (2.43). Solving the resulting system of equations, we find the trigonometric functions of the rotation angle ζ

$$\cos\zeta = \frac{\varepsilon_0}{\Delta E}, \quad \sin\zeta = \frac{\Delta}{\Delta E}. \tag{2.44}$$

From simple trigonometric transformations, we find similar functions of the half-angle

$$\cos\frac{\zeta}{2} = \gamma_+ = \frac{1}{\sqrt{2}}\sqrt{1+\frac{\varepsilon_0}{\Delta E}}, \tag{2.45}$$

$$\sin\frac{\zeta}{2} = \gamma_- = \frac{1}{\sqrt{2}}\sqrt{1-\frac{\varepsilon_0}{\Delta E}}. \tag{2.46}$$

Thus, we were able to express the rotation matrix from (2.41) through the parameters of the Hamiltonian. Given that the basis vectors, unlike wave functions, are transformed using the direct matrix (2.41), we can express the new basis vectors $\{|E_-\rangle, |E_+\rangle\}$ through the old ones $\{|0\rangle, |1\rangle\}$ as

$$|E_-\rangle = \cos\frac{\zeta}{2}|0\rangle + \sin\frac{\zeta}{2}|1\rangle = \gamma_+|0\rangle + \gamma_-|1\rangle, \tag{2.47}$$

$$|E_+\rangle = \sin\frac{\zeta}{2}|0\rangle - \cos\frac{\zeta}{2}|1\rangle = \gamma_-|0\rangle - \gamma_+|1\rangle. \tag{2.48}$$

As we can see, up to a phase factor, the latter expressions (2.47)-(2.48) coincide with those obtained earlier (2.38)-(2.39), which is the expected result.

SECTION 3. USING RABI OSCILLATIONS FOR QUBIT STATE CONTROL

Within this section, it will be shown exactly how and under what conditions Rabi oscillations occur, and the reasons for their main drawbacks will be analyzed in detail. An important part also includes the derivation of the phenomenological Bloch equation, which describes the dissipative influence of the environment on the system.

3.1 Rabi oscillations as a method of changing the qubit state

Let us consider a two-level system and the simplest case of an alternating magnetic field – harmonic oscillations of the z-coordinate of the intensity. In this case, the general Hamiltonian of the system depends on time and coincides with formula (2.31). Using its known expression, one can formulate the Schrödinger equation and examine the evolution of the system in detail. An interesting result is that, given certain field parameters, situations periodically arise where the qubit is in one of the basis states with a probability of one. This phenomenon is called Rabi oscillations [5].

For further calculations, it also proves important to introduce the concept of the qubit's resonant frequency ω_q. Essentially, this is the frequency a photon must have so that its energy is sufficient to excite an electron and transition from the lower energy level $|E_-\rangle$ to the upper one $|E_+\rangle$:

$$\omega_q = \frac{\Delta E}{\hbar}. \tag{3.1}$$

Obviously, the qubit can transition to another energy level by absorbing or emitting a larger number of photons simultaneously, so we will take this into account.

Let us consider a more general case when the magnetic field is quite strong. We formulate this mathematically in the form of the following two conditions:

$$k\hbar\omega \sim \Delta E = \hbar\omega_q,\ k \in \mathbb{Z}, \tag{3.2}$$

$$\Delta \ll \sqrt{A\hbar\omega}. \tag{3.3}$$

The first of these conditions indicates the multiplicity of the qubit's resonant frequency to the frequency of the applied field. The second states that the constant field component is much smaller than the given set of parameters. The specific form of this condition will be explained later.

Let us now move to a more convenient frame of reference. To do this, we will consider a rotating coordinate system, i.e., we will use the following operator as a rotation matrix:

$$U(t) = \exp\left(-\frac{i}{\hbar}\int V(t)dt\right) \equiv \exp\left(i\frac{\eta(t)}{2}\sigma_z\right) = \cos\left(\frac{\eta}{2}\right) + i\sigma_z \sin\left(\frac{\eta}{2}\right), \tag{3.4}$$

where $\eta(t)$ is the time-dependent rotation angle. Let us calculate it directly using the substitution of the expression for $V(t)$ from formula (2.31):

$$-\frac{i}{\hbar}\int V(t)dt = -\frac{i}{\hbar}\int_0^t -\frac{A\cos\omega t}{2}\sigma_z dt = \frac{iA\sin\omega t}{2\hbar\omega}\sigma_z = i\frac{\eta(t)}{2}\sigma_z \rightarrow$$
$$\rightarrow \eta(t) = \frac{A}{\hbar\omega}\sin\omega t. \tag{3.5}$$

In fact, the operator $U(t)$ connects the wave functions in the stationary $|\psi\rangle$ and rotating $|\psi'\rangle$ systems. Let us write the formula for their connection, as well as the Schrödinger equation in both systems:

$$|\psi\rangle = U(t)\,|\psi'\rangle, \quad i\hbar|\dot{\psi}\rangle = H\,|\psi\rangle, \quad i\hbar|\dot{\psi}'\rangle = H'\,|\psi'\rangle \tag{3.6}$$

Making mutual substitutions, we can find the expression for the Hamiltonian H' in the new system:

$$\begin{gathered} i\hbar U|\dot{\psi}'\rangle + i\hbar\dot{U}\,|\psi'\rangle = HU\,|\psi'\rangle \rightarrow i\hbar U|\dot{\psi}'\rangle = (HU - i\hbar\dot{U})\,|\psi'\rangle \rightarrow \\ i\hbar|\dot{\psi}'\rangle = (U^{-1}HU - i\hbar U^{-1}\dot{U})\,|\psi'\rangle \rightarrow H' = U^{-1}HU - i\hbar U^{-1}\dot{U} \end{gathered} \tag{3.7}$$

we can calculate the derivative of the operator $U(t)$ from its definition (3.4). We get the result

$$\dot{U} = -\frac{i}{\hbar}VU. \tag{3.8}$$

In addition, we use the unitarity of this operator ($U^{-1} = U^{\dagger}$) to perform the following transformations:

$$H' = U^{\dagger}HU - U^{\dagger}VU = U^{\dagger}(H - V)U = U^{\dagger}H_0U. \tag{3.9}$$

Multiplying the matrices (3.4) and (2.31), we find the explicit form of the new Hamiltonian:

$$H' = -\frac{1}{2}\begin{pmatrix} \varepsilon_0 & \Delta e^{-i\eta} \\ \Delta e^{i\eta} & \varepsilon_0 \end{pmatrix} = -\frac{\Delta}{2}(e^{-i\eta}\sigma_+ + e^{i\eta}\sigma_-) - \frac{\varepsilon_0}{2}\sigma_z \tag{3.10}$$

For convenience of notation, two operators $\sigma_\pm$, related to the Pauli matrices, were used here. They are defined as follows:

$$\sigma_\pm = \frac{1}{2}(\sigma_x \pm i\sigma_y) \to \sigma_+ = \begin{pmatrix} 0 & 1 \\ 0 & 0 \end{pmatrix}, \quad \sigma_- = \begin{pmatrix} 0 & 0 \\ 1 & 0 \end{pmatrix}. \tag{3.11}$$

As we can see, the obtained Hamiltonian from formula (3.10) contains the terms $e^{\pm i\eta}$, which have a sine in the exponent (see formula (3.5)). This allows us to use the Jacobi-Anger expansion [33]. In general form, such an exponential can be represented as

$$e^{ix\sin\tau} = \sum_{n=-\infty}^{\infty} J_n(x)e^{in\tau}, \tag{3.12}$$

where $J_n(x)$ is the Bessel function of the first kind. By definition, it can be written as

$$J_n(x) = \sum_{m=0}^{\infty} \frac{(-1)^m}{m!\Gamma(m+n+1)}\left(\frac{x}{2}\right)^{2m+n}, \tag{3.13}$$

where $\Gamma(x)$ is the gamma function.

Applying the expansion (3.12) to the terms with $e^{\pm i\eta}$, we get:

$$e^{\pm i\eta} = \sum_{n=-\infty}^{\infty} J_n\left(\frac{A}{\hbar\omega}\right)e^{\pm in\omega t}. \tag{3.14}$$

Substituting these expressions into (3.10), we find the system's Hamiltonian in the most convenient form for further work:

$$H' = -\sum_{n=-\infty}^{\infty} \frac{\Delta_n}{2}(e^{-in\omega t}\sigma_+ + e^{in\omega t}\sigma_-) - \frac{\varepsilon_0}{2}\sigma_z, \tag{3.15}$$

where $\Delta_n = \Delta J_n\left(\frac{A}{\hbar\omega}\right)$ is another introduced notation.

As already noted, this Hamiltonian describes the behavior of a qubit in a moving system. Considering that it contains an infinite number of harmonics, it becomes obvious that it is impossible to obtain an analytical solution to the Schrödinger equation with a Hamiltonian of this form. Therefore, a solution in quadratures can only be obtained in a certain approximation.

As we can see, all exponentials from expression (3.15) can be divided into fast (when $n \geq 1$) and slowly oscillating (when $n = 0$). This potentially makes it possible to use the so-called Rotating-Wave Approximation (RWA) [34]. It consists of neglecting the fast terms in the resulting rotating system (interaction picture). Since in our case we are considering the case of a strong field, let's recall condition (3.3). It was introduced to ensure the smallness of the coefficients in front of the exponentials, which follows from perturbation theory and is necessary for the applicability of the RWA. Considering that $J_n \leq 1$, the necessary condition precisely becomes a small value of the parameter Δ, which was postulated in (3.3).

So, we can try to use this approximation. To do this, let's also transition to the moving frame of the k-th harmonic:

$$|\psi''\rangle = \exp\left(i\frac{k\omega t}{2}\sigma_z\right)|\psi'\rangle \rightarrow |\psi'\rangle = \exp\left(-i\frac{k\omega t}{2}\sigma_z\right)|\psi''\rangle \rightarrow \begin{pmatrix} a' \\ b' \end{pmatrix} = \begin{pmatrix} e^{-i\frac{k\omega t}{2}}a'' \\ e^{i\frac{k\omega t}{2}}b'' \end{pmatrix}, \tag{3.16}$$

where $|\psi'\rangle = (a', b')^{\mathsf{T}}$, $|\psi''\rangle = (a'', b'')^{\mathsf{T}}$.

From a physical point of view, this transition means that in the resulting system, the case of the qubit absorbing k photons with a subsequent transition to another energy level becomes resonant. Mathematically, this is manifested in the fact that the corresponding term of the sum becomes stationary (contains $e^{\pm i0\omega t} \sim 1$). Let's show this explicitly:

$$H'|\psi'\rangle = \left(-\sum_{n=-\infty}^{\infty}\frac{\Delta_n}{2}(e^{-in\omega t}\sigma_+ + e^{in\omega t}\sigma_-) - \frac{\varepsilon_0}{2}\sigma_z\right)\exp\left(-i\frac{k\omega t}{2}\sigma_z\right)\begin{pmatrix} a'' \\ b'' \end{pmatrix}, \tag{3.17}$$

$$i\hbar|\dot{\psi}'\rangle = i\hbar\exp\left(-i\frac{k\omega t}{2}\right)\left(\begin{pmatrix} \dot{a}'' \\ \dot{b}'' \end{pmatrix} - i\frac{k\omega}{2}\begin{pmatrix} a'' \\ -b'' \end{pmatrix}\right), \tag{3.18}$$

$$i\hbar\begin{pmatrix}\dot{a}''\\ \dot{b}''\end{pmatrix}=-\sum_{n=-\infty}^{\infty}\frac{\Delta_n}{2}\begin{pmatrix}b''e^{i\omega t(k-n)}\\ a''e^{-i\omega t(k-n)}\end{pmatrix}-\frac{k\hbar\omega}{2}\begin{pmatrix}a''\\ -b''\end{pmatrix}-\frac{\varepsilon_0}{2}\begin{pmatrix}a''\\ -b''\end{pmatrix}. \quad (3.19)$$

Indeed, the term of the sum with $k = n$ becomes constant, and the others will be rapidly oscillating compared to it. Using the rotating-wave approximation, we discard them. Thus, from equation (3.15) we obtain a simplified system, which can now be solved analytically (here and below, for notational convenience, $a'' = a$, $b'' = b$ are denoted):

$$\begin{pmatrix}\dot{a}\\ \dot{b}\end{pmatrix}=i\frac{\Delta_k}{2\hbar}\begin{pmatrix}b\\ a\end{pmatrix}+\frac{i}{2\hbar}(k\hbar\omega+\varepsilon_0)\begin{pmatrix}a\\ -b\end{pmatrix}. \quad (3.20)$$

The next step is solving the derived system. Given its bulkiness, we will not present it entirely but will show only the main results. First, we express $a(t)$ through $b(t)$, which gives us a 2nd-order ODE with constant coefficients:

$$\ddot{b}+\frac{\Delta_k^2+(k\hbar\omega+\varepsilon_0)^2}{4\hbar^2}b=0. \quad (3.21)$$

It is easily solved analytically. To do this, we make, for example, the substitution $b = \exp(i\lambda t)$, after which (3.21) turns into a quadratic equation for λ. From it we find that

$$\lambda_{1,2}^{(k)}=\pm\frac{1}{2\hbar}\sqrt{\Delta_k^2+(k\hbar\omega+\varepsilon_0)^2}. \quad (3.22)$$

This gives us expressions for $b(t)$ and $a(t)$:

$$b_{1,2}^{(k)}=B_{1,2}^{(k)}e^{i\lambda_{1,2}^{(k)}t}, \quad (3.23)$$

$$a_{1,2}^{(k)}=A_{1,2}^{(k)}e^{i\lambda_{1,2}^{(k)}t}=\frac{2\hbar\lambda_{1,2}^{(k)}+(k\hbar\omega+\varepsilon_0)}{\Delta_k}B_{1,2}^{(k)}e^{i\lambda_{1,2}^{(k)}t}, \quad (3.24)$$

where $B_{1,2}^{(k)}$, $A_{1,2}^{(k)}$ are some constants, which are found from the normalization condition

$$|a_{1,2}^{(k)}|^2+|b_{1,2}^{(k)}|^2=1. \quad (3.25)$$

The coefficients themselves are equal to

$$B_{1,2}^{(k)} = \frac{\Delta_k}{\sqrt{\Delta_k^2 + \left(2\hbar\lambda_{1,2}^{(k)} + (k\hbar\omega + \varepsilon_0)\right)^2}}, \tag{3.26}$$

$$A_{1,2}^{(k)} = \frac{2\hbar\lambda_{1,2}^{(k)} + (k\hbar\omega + \varepsilon_0)}{\sqrt{\Delta_k^2 + \left(2\hbar\lambda_{1,2}^{(k)} + (k\hbar\omega + \varepsilon_0)\right)^2}}. \tag{3.27}$$

Let us analyze the obtained results. Using formulas (3.23)-(3.25) and (3.16), we can build a new basis of wave functions

$$|\psi_{1,2}^{(k)}\rangle = \begin{pmatrix} a_{1,2}^{(k)} e^{-i\frac{k\omega}{2}t} \\ b_{1,2}^{(k)} e^{i\frac{k\omega}{2}t} \end{pmatrix} = e^{i\lambda_{1,2}^{(k)}t} \begin{pmatrix} A_{1,2}^{(k)} e^{-i\frac{k\omega}{2}t} \\ B_{1,2}^{(k)} e^{i\frac{k\omega}{2}t} \end{pmatrix}. \tag{3.28}$$

Now we have an expression for the wave function $|\psi\rangle$ in two bases:

$$|\psi\rangle = C_1 |\psi_1^{(k)}\rangle + C_2 |\psi_2^{(k)}\rangle = C_- |E_-\rangle + C_+ |E_+\rangle = \begin{pmatrix} C_- \\ C_+ \end{pmatrix}. \tag{3.29}$$

The next calculation step will be finding the coefficients $C_{1,2}$ in the new basis. In the general case, this is a tedious task, but by choosing convenient initial conditions, the problem can be simplified. So let the qubit be at the lower energy level at the initial moment of time:

$$|\psi(t=0)\rangle = |E_-\rangle. \tag{3.30}$$

Thus we obtain a new system of equations for the unknowns $C_{1,2}$:

$$\begin{cases} C_1 A_1^{(k)} + C_2 A_2^{(k)} = 1, \\ C_1 B_1^{(k)} + C_2 B_2^{(k)} = 0. \end{cases} \tag{3.31}$$

To solve it, we will use (without proof) the relation $B_2^{(k)}A_1^{(k)} - B_1^{(k)}A_2^{(k)} = 1$. This allows us to rewrite the newly obtained system and find the required coefficients $C_{1,2}$:

$$\begin{cases} C_1A_1^{(k)} + C_2A_2^{(k)} = B_2^{(k)}A_1^{(k)} - B_1^{(k)}A_2^{(k)}, \\ C_1B_1^{(k)} + C_2B_2^{(k)} = 0, \end{cases} \rightarrow \begin{cases} C_1 = B_2^{(k)}, \\ C_2 = -B_1^{(k)}. \end{cases} \tag{3.32}$$

Finally, this can be rewritten in the following form to explicitly extract the expressions for the coefficients $C_{\mp}$ from formula (3.29):

$$\begin{pmatrix} C_- \\ C_+ \end{pmatrix} = B_2^{(k)}e^{i\lambda_1^{(k)}t}\begin{pmatrix} A_1^{(k)}e^{-i\frac{k\omega}{2}t} \\ B_1^{(k)}e^{i\frac{k\omega}{2}t} \end{pmatrix} - B_1^{(k)}e^{i\lambda_2^{(k)}t}\begin{pmatrix} A_2^{(k)}e^{-i\frac{k\omega}{2}t} \\ B_2^{(k)}e^{i\frac{k\omega}{2}t} \end{pmatrix}, \tag{3.33}$$

in particular

$$C_+ = B_1^{(k)}B_2^{(k)}\left(e^{i\lambda_1^{(k)}t} - e^{-i\lambda_1^{(k)}t}\right)e^{i\frac{k\omega}{2}t}. \tag{3.34}$$

As a result, the probability of being in the state $|E_+\rangle$ at some time t will be:

$$P_+^{(k)}(t) = |C_+|^2 = 2B_1^{(k)2}B_2^{(k)2}(1 - \cos 2\lambda_1^{(k)}t). \tag{3.35}$$

Let us now introduce the concept of the generalized Rabi frequency for a k-photon resonance:

$$\Omega_{R,k} = 2\lambda_1^{(k)} = \frac{1}{\hbar}\sqrt{\Delta_k^2 + (k\hbar\omega + \varepsilon_0)^2}. \tag{3.36}$$

Obviously, its dimension corresponds to the dimension of frequencies. We substitute it into formula (3.35), which gives us

$$P_+^{(k)}(t) = |C_+|^2 = 2B_1^{(k)2}B_2^{(k)2}(1 - \cos \Omega_{R,k}t). \tag{3.37}$$

Let us analyze the obtained result. The probabilities of being at each of the energy levels change according to a harmonic law with the Rabi frequency $\Omega_{R,k}$. This reveals the physical meaning of this quantity as the oscillation frequency of the probabilities $P_{\pm}^{(k)}(t)$. Let us now try to calculate the average populations of the energy levels. To do this, we

average $P_+^{(k)}$ over the Rabi period $T_R = \frac{2\pi}{\Omega_R}$:

$$\overline{P_+^{(k)}} = \frac{1}{T_R}\int_0^{T_R} dt P_+^{(k)}(t) = 2B_1^{(k)2}B_2^{(k)2} = \frac{1}{2}\frac{\Delta_k^2}{\Delta_k^2 + (k\hbar\omega + \varepsilon_0)^2}. \quad (3.38)$$

Thus, if the system is in exact resonance (i.e., condition (3.2) is fulfilled), then and only then both Rabi frequencies become equal (because given the smallness of Δ, one can use the approximation $k\hbar\omega = \Delta E \approx -|\varepsilon_0|$). The minus sign arises due to the fact that when $|\varepsilon_0| = -\varepsilon_0$, this indicates the process of absorbing $k > 0$ photons, and vice versa. Expression (3.37) simplifies even further:

$$P_+^{(k)}(t) = \overline{P_{+max}^{(k)}}(1 - \cos\Omega_{R,k}t) = \frac{1 - \cos\Omega_{R,k}t}{2}. \quad (3.39)$$

Considering that the cosine takes values from -1 to 1, it is easy to understand that there will be moments when $P_+^{(k)}(t) = 1$ and $P_+^{(k)}(t) = 0$ (i.e., $P_-^{(k)}(t) = 1$). Therefore, during the qubit's evolution, there are indeed moments when it is guaranteed to be in one of the basis states, which can be used to create quantum gates.

Let us conduct further analysis. The fact that $\overline{P_+^{(k)}} \leq \frac{1}{2}$ means it is impossible to create a population inversion of the qubit. We will also additionally consider the situation when $A \ll \hbar\omega$ (the case of a weak field within this model). This limitation allows using the asymptotics of the Bessel function $J_k \approx \frac{x^k}{2^k k!}$ (follows from formula (3.13)). In particular, for a single-photon transition, i.e., $k = 1$, the Rabi oscillation frequency at resonance will be:

$$\Omega_{R,1} = 2\lambda_1^{(1)} = \frac{1}{\hbar}\sqrt{\Delta_1^2 + (\hbar\omega - |\varepsilon_0|)^2} = \frac{\Delta_1}{\hbar} \approx \frac{\Delta A}{2\hbar^2\omega} \approx \frac{\Delta A}{2\hbar\Delta E}. \quad (3.40)$$

The last thing to note within this topic is that in the case of a weak field $J_1\left(\frac{A}{\hbar\omega}\right) \sim \frac{A}{\hbar\omega} \ll \left(\frac{A}{\hbar\omega}\right)^n \sim J_k\left(\frac{A}{\hbar\omega}\right)$ for $k > 1$. This means that the Rabi frequencies for multi-photon excitations are significantly lower than for single-photon ones (since $\Omega_{R,1} \sim \Delta_1 \ll \Delta_k \sim \Omega_{R,k}$). Such transitions occur very slowly, so under the condition $A \ll \hbar\omega$ they can be neglected. In particular, Fig. 3.1 demonstrates that the approximate and exact numerical solutions for $P_+(t)$ in the case of a weak field almost completely coincide.

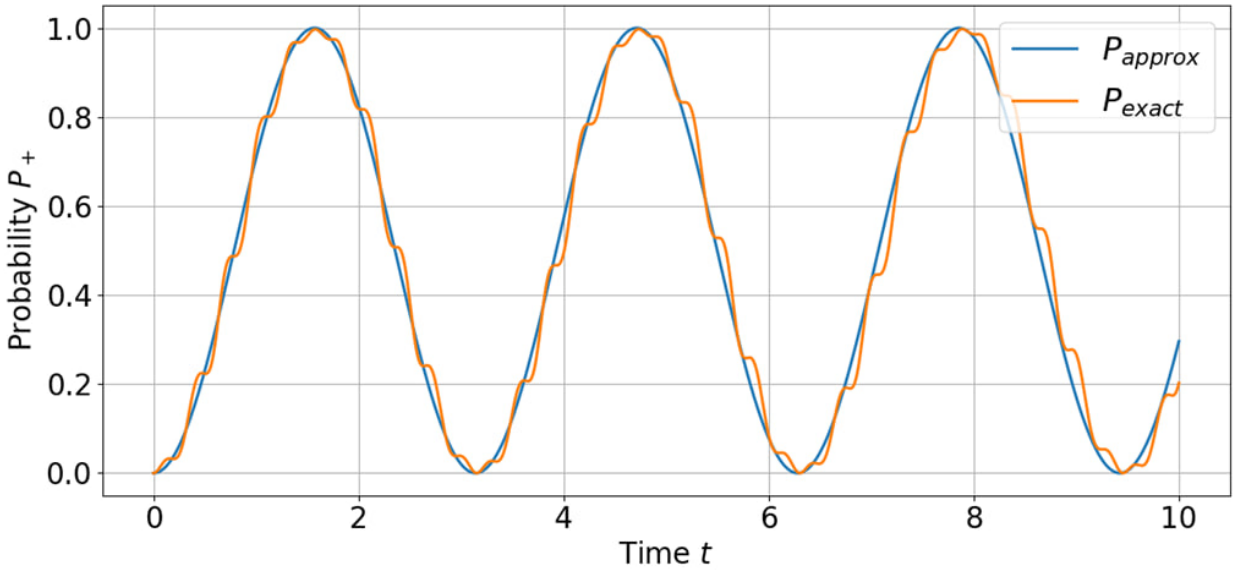

Figure 3.1 – Exact and approximate form of Rabi oscillations (probabilities)

Thus, the equation of probability oscillations was obtained for two limiting cases – strong and weak fields.

3.2 Accounting for relaxation processes during the system's evolution. Bloch equations

All derivations in 3.1 were made assuming that our quantum system is isolated and does not interact with a dissipative environment. Now we will try to account for its influence. We will consider the relaxation process phenomenologically. In an idealized system where interaction with a reservoir is absent, the Liouville-von Neumann equation (2.26) formally coincides with the Bloch equations. Nevertheless, to describe real systems, it is necessary to introduce an additional term into this equation that would provide exponential decay:

$$\dot{\rho}_{ij} = -\frac{i}{\hbar}[H,\rho]_{ij} - \frac{\rho_{ij} - \rho_{ij}^{(0)}}{\tau_{ij}}, \tag{3.41}$$

where τ_{ij} is some characteristic time, $\rho_{ij}^{(0)}$ are the elements of the equilibrium density matrix.

It is easy to verify that the introduced term indeed yields a solution in the form of a decaying exponential:

$$\dot{\rho}_{ij} = -\frac{\rho_{ij} - \rho_{ij}^{(0)}}{\tau_{ij}} \to d\Big(\ln\Big(\rho_{ij} - \rho_{ij}^{(0)}\Big)\Big) = -\frac{dt}{\tau_{ij}} \to \rho_{ij}(t) = \rho_{ij}^{(0)} + Ce^{-\frac{t}{\tau_{ij}}}. \quad (3.42)$$

Let the system be in thermal equilibrium with the environment at some temperature T. From statistical physics [35], the equilibrium value of the density operator is known:

$$\rho^{(0)} = \frac{1}{\Sigma}\exp\left(-\frac{H_0}{kT}\right), \quad (3.43)$$

where Σ is the partition function, and k is the Boltzmann constant.

From property (2.16) it follows that

$$\mathrm{Tr}\,\rho^{(0)} = \mathrm{Tr}\left(\frac{1}{\Sigma}e^{-\frac{H_0}{kT}}\right) = \frac{1}{\Sigma}\mathrm{Tr}\left(e^{-\frac{H_0}{kT}}\right) = 1 \to \Sigma = \mathrm{Tr}\left(e^{-\frac{H_0}{kT}}\right). \quad (3.44)$$

Using formula (2.18), we now find individual elements of the density matrix:

$$\begin{cases}\rho_{00,11}^{(0)} = \frac{1}{\Sigma}\langle E_{\mp}|\, e^{-\frac{H_0}{kT}}\,|E_{\mp}\rangle, \\ \rho_{10,01}^{(0)} = \frac{1}{\Sigma}\langle E_{\pm}|\, e^{-\frac{H_0}{kT}}\,|E_{\mp}\rangle, \end{cases} \to \begin{cases}\rho_{00,11}^{(0)} = \frac{1}{\Sigma}e^{-\frac{E_{\mp}}{kT}}\langle E_{\mp}|E_{\mp}\rangle, \\ \rho_{10,01}^{(0)} = \frac{1}{\Sigma}e^{-\frac{E_{\mp}}{kT}}\langle E_{\pm}|E_{\mp}\rangle, \end{cases} \to \begin{cases}\rho_{00,11}^{(0)} = \frac{1}{\Sigma}e^{\pm\frac{\Delta E}{2kT}}, \\ \rho_{10,01}^{(0)} = 0. \end{cases} \quad (3.45)$$

Let us reflect on the obtained results from a physics perspective. It is expected that the state populations $\rho_{00,11}^{(0)}$ are determined by the Boltzmann distribution. This also gives us the opportunity to use another method for finding the normalization constant Σ, which consists of applying condition (2.19):

$$\rho_{00}^{(0)} + \rho_{11}^{(0)} = 1 \to \frac{1}{\Sigma}\left(e^{-\frac{\Delta E}{2kT}} + e^{\frac{\Delta E}{2kT}}\right) = 1 \to \Sigma = 2\cosh\frac{\Delta E}{2kT} \quad (3.46)$$

In general, there are two main consequences of the long-term interaction of the system with the environment – a return to the state with the lowest energy (energy loss) and the disappearance of such qubit properties as superposition and entanglement (phase loss). Also, in 2.2.2 it was established that the system being at a certain energy level is mathemat-

ically described using $\rho_{00,11}$, and the phase relationship between these levels is embedded in the elements $\rho_{10,01}$. Thus, the physical meaning of τ_{ij} differs for the diagonal and off-diagonal elements of the density matrix. Therefore, it is necessary to introduce two new quantities – $\tau_{ii} = T_1$ (energy relaxation time) and $\tau_{ij} = T_2$, where $i \neq j$ (decoherence time), and in the general case $T_1 > T_2$.

Consider how to find the general form of the elements of the density operator. We use the previously derived Hamiltonian of the system in the rotating-wave approximation (see formula (3.15)) for the k-photon resonance (all terms with $k \neq n$ vanish) and find the value of the commutator $[H, \rho]$:

$$[H,\rho] = -\frac{1}{2}\begin{pmatrix} \varepsilon_0 & \Delta_k e^{-ik\omega t} \\ \Delta_k e^{-ik\omega t} & \varepsilon_0 \end{pmatrix}\begin{pmatrix} \rho_{00} & \rho_{01} \\ \rho_{10} & \rho_{11} \end{pmatrix} + \\ + \frac{1}{2}\begin{pmatrix} \rho_{00} & \rho_{01} \\ \rho_{10} & \rho_{11} \end{pmatrix}\begin{pmatrix} \varepsilon_0 & \Delta_k e^{-ik\omega t} \\ \Delta_k e^{-ik\omega t} & \varepsilon_0 \end{pmatrix} =$$

$$= -\frac{1}{2}\begin{pmatrix} \Delta_k(e^{-ik\omega t}\rho_{10} - e^{ik\omega t}\rho_{01}) & 2\varepsilon_0\rho_{01} + \Delta_k e^{-ik\omega t}(\rho_{11} - \rho_{00}) \\ -2\varepsilon_0\rho_{10} + \Delta_k e^{ik\omega t}(\rho_{00} - \rho_{11}) & \Delta_k(e^{ik\omega t}\rho_{01} - e^{-ik\omega t}\rho_{10}) \end{pmatrix}. \quad (3.47)$$

Substituting this into formula (3.41), we can compile the following system of equations:

$$\begin{cases} \dot{\rho}_{00} = \frac{i}{2\hbar}\Delta_k(e^{-ik\omega t}\rho_{10} - e^{ik\omega t}\rho_{01}) - \frac{\rho_{00}-\rho_{00}^{(0)}}{T_1}, \\ \dot{\rho}_{11} = \frac{i}{2\hbar}\Delta_k(e^{ik\omega t}\rho_{01} - e^{-ik\omega t}\rho_{10}) - \frac{\rho_{11}-\rho_{11}^{(0)}}{T_1}, \\ \dot{\rho}_{10} = -\frac{i}{\hbar}\varepsilon_0\rho_{10} + i\frac{\rho_{00}-\rho_{11}}{2\hbar}\Delta_k e^{ik\omega t} - \frac{\rho_{10}}{T_2}, \\ \dot{\rho}_{01} = \frac{i}{\hbar}\varepsilon_0\rho_{01} + i\frac{\rho_{11}-\rho_{00}}{2\hbar}\Delta_k e^{-ik\omega t} - \frac{\rho_{01}}{T_2}. \end{cases} \quad (3.48)$$

From the properties of the density operator (2.15), (2.16), it is known that not all of its elements are independent, so the number of equations can be reduced. Besides, it may turn out to be convenient to describe the system's evolution not directly in terms of the elements ρ_{ij}, but through the coordinates of the Bloch vector $\vec{R}$. It is easy to verify that

$$\rho = \frac{1}{2}(I + \vec{R}\vec{\sigma}) = \begin{pmatrix} 1+Z & X-iY \\ X+iY & 1-Z \end{pmatrix} \equiv \begin{pmatrix} \rho_{00} & \rho_{01} \\ \rho_{10} & \rho_{11} \end{pmatrix}, \quad (3.49)$$

where $\vec{R} = (X, Y, Z)$ are the coordinates of the Bloch vector.

From here it follows that

$$Z^{(0)} = \frac{1 + Z^{(0)}}{2} - \frac{1 - Z^{(0)}}{2} = \rho_{00}^{(0)} - \rho_{11}^{(0)} = \frac{1}{\Sigma}\left(e^{-\frac{\Delta E}{2kT}} - e^{\frac{\Delta E}{2kT}}\right) = \\ = \frac{2}{\Sigma}\sinh\frac{\Delta E}{2kT} = \tanh\frac{\Delta E}{2kT}. \quad (3.50)$$

Combining the first two equations from (3.48) into one, removing another one due to the Hermiticity of the density operator equation for $\dot{\rho}_{01}$, and making some other simplifications, we obtain the system

$$\begin{cases} \dot{Z} = i\frac{\Delta_k}{\hbar}(e^{-ik\omega t}\rho_{10} - e^{ik\omega t}\rho_{01}) - \frac{Z - Z^{(0)}}{T_1}, \\ \dot{\rho}_{10} = -i\frac{\varepsilon_0}{\hbar}\rho_{10} + i\frac{\Delta_k}{2\hbar}e^{ik\omega t}Z - \frac{\rho_{10}}{T_2}. \end{cases} \quad (3.51)$$

As with $\rho_{00,11}$, we make a substitution to express the off-diagonal elements $\rho_{01,10}$ through the reduced coordinates of the Bloch vector $\tilde{X}$, $\tilde{Y}$ in the rotating frame

$$\rho_{10}\exp(-ik\omega t) = \frac{1}{2}(\tilde{X} + i\tilde{Y}). \quad (3.52)$$

Making the final transformations, we get a system of three equations:

$$\begin{cases} \dot{\tilde{X}} = \left(k\omega + \frac{\varepsilon_0}{\hbar}\right)\tilde{Y} - \frac{\tilde{X}}{T_2}, \\ \dot{\tilde{Y}} = -\left(k\omega + \frac{\varepsilon_0}{\hbar}\right)\tilde{X} + \frac{\Delta_k}{\hbar}Z - \frac{\tilde{Y}}{T_2}, \\ \dot{Z} = -\frac{\Delta_k}{\hbar}\tilde{Y} - \frac{Z - Z^{(0)}}{T_1}. \end{cases} \quad (3.53)$$

The solution of this system in the general case is quite complex. So we will limit ourselves to considering the equilibrium state of the qubit, i.e., we will look for a solution at the moment $t \gg T_1, T_2$. Effectively, this means that the qubit state in the rotating frame of the k-photon resonance (in which the chosen Hamiltonian (3.15) is written) does not change over time. Note that in this system, the Bloch vector has coordinates $\vec{\tilde{R}} = (\tilde{X}, \tilde{Y}, Z)$. The corresponding transition to the moving resonant system for the first two coordinates was shown in formula (3.52), and the rotation does not affect the last coordinate at all,

because it occurs exactly around the z axis. As a consequence, in the equilibrium state, the system of equations (3.53) looks like

$$\dot{\vec{\tilde{R}}} = 0 \to \begin{cases} \left(k\omega + \frac{\varepsilon_0}{\hbar}\right)\tilde{Y} - \frac{\tilde{X}}{T_2} = 0, \\ \left(k\omega + \frac{\varepsilon_0}{\hbar}\right)\tilde{X} + \frac{\Delta_k}{\hbar}Z - \frac{\tilde{Y}}{T_2} = 0, \\ -\frac{\Delta_k}{\hbar}\tilde{Y} - \frac{Z - Z^{(0)}}{T_1} = 0. \end{cases} \tag{3.54}$$

Solving it now, we get the following result:

$$Z = Z^{(0)} \frac{\frac{T_2}{T_1}(k\omega\hbar + \varepsilon_0)^2 + \frac{\hbar^2}{T_1 T_2}}{\Delta_k^2 + \frac{T_2}{T_1}(k\omega\hbar + \varepsilon_0)^2 + \frac{\hbar^2}{T_1 T_2}} \tag{3.55}$$

Now we can find the population of the upper energy level as well. To do this, we substitute the newly derived expression into formula (3.50). Additionally, we assume that the reservoir temperature is quite low. This corresponds to an equilibrium state with $\rho_{11}^{(0)} = \frac{1}{2}(1 - Z^{(0)}) \approx 0$, which allows equating $Z^{(0)} \approx 1$. Therefore, the average probability of a k-photon excitation is

$$\overline{P}_+^{(k)} = \overline{\rho_{11}}^{(k)} = \frac{1}{2}(1 - \overline{Z}^{(k)}) = \frac{1}{2}\frac{\Delta_k^2}{\Delta_k^2 + \frac{T_2}{T_1}(k\omega\hbar + \varepsilon_0)^2 + \frac{\hbar^2}{T_1 T_2}}. \tag{3.56}$$

Obviously, the total average probability of finding the qubit in an excited state under the condition of the system's equilibrium with the environment is calculated as the sum of $\overline{P}_+^{(k)}$ over different values of k:

$$\overline{P}_+(\varepsilon_0, A) = \sum_k \overline{P}_+^{(k)} = \frac{1}{2}\sum_k \frac{\Delta_k^2}{\Delta_k^2 + \frac{T_2}{T_1}(k\omega\hbar + \varepsilon_0)^2 + \frac{\hbar^2}{T_1 T_2}}. \tag{3.57}$$

Let us consider another limiting case when $T_1 = T_2 \to \infty$. Technically, this approximation means the absence of relaxation. At the same time, the expression for $\overline{P}_+^{(k)}$ simplifies to the form

$$\overline{P}_+^{(k)} = \frac{1}{2}\frac{\Delta_k^2}{\Delta_k^2 + (k\omega\hbar + \varepsilon_0)^2}. \tag{3.58}$$

The obtained result expectedly coincides with formula (3.38), which was obtained in 3.1 without taking relaxation into account, which confirms the correctness of the calculations.

3.3 Drawbacks of the Rabi method

As already discussed in 1.2, executing logical operations on qubits using Rabi oscillations is accompanied by significant problems. Despite the simplicity and intuitive clarity of this approach, it has a number of significant physical and hardware limitations. Let us now analyze why this method has such drawbacks at all, relying on the presented mathematical apparatus in 3.1. In particular, they include:

1) a strict correlation between the gate speed and the approximation accuracy. This follows from formula (3.40). As we can see, the oscillation frequency is determined by the amplitude of the external driving field A and is directly proportional to the operation execution speed. That is, to make the gate faster, it is necessary to increase this parameter A. However, then the RWA starts to be violated because the magnetic field ceases to be weak, which further manifests in an increase in errors;

2) the experimental complexity of controlling the field parameters. This also follows from formula (3.40). Since the probability of the system being in an excited state is determined through the oscillation frequency $\Omega_{R,k}$, for the accurate execution of a logical gate, it is necessary to perfectly tune and maintain the amplitude value of the electromagnetic pulse. But experimentally setting the field amplitude with ultra-high precision is much more difficult than controlling its frequency. Therefore, any instrumental errors automatically lead to a significant (within the scope of the given task) unwanted change in the qubit's state;

3) population leakages (leakage) outside the qubit subspace. Gates based on Rabi oscillations are implemented strictly at resonant frequencies ω_q, when the energy detuning is minimal ($\omega - \omega_q \ll \omega$). However, in practice, multi-level quantum systems are not ideal two-level ones. In them, the energy distance between successive sublevels is also quite close to the resonant frequency ω_q. As a result, large-amplitude resonant excitation can cause population leakages to these higher levels. This takes the system out of the working qubit space, information is irretrievably lost, and the gate fidelity drops.

Thus, the method of controlling a qubit state using Rabi oscillations, although quite simple, indeed has significant problems. This does not make it completely unusable, but forces the search for higher-precision alternatives.

SECTION 4. USING LZSM TRANSITIONS FOR QUBIT STATE CONTROL

This section discusses an alternative non-resonant non-adiabatic approach to qubit control. In addition to a direct explanation of this effect, the end of the section describes the methodology for selecting control parameters to perform an arbitrary unitary quantum operation.

4.1 Reasons for the occurrence of LZSM transitions. Single passage

Let us consider the simplest single-qubit system located in an alternating magnetic field that changes according to a harmonic law

$$\varepsilon(t) = \varepsilon_0 + A \sin \omega t. \tag{4.1}$$

Then its energy levels will also change periodically (see Fig. 4.1). An interesting fact is that, depending on the choice of basis, they will either cross (in the diabatic $\{|1\rangle, |0\rangle\}$) or not (in the adiabatic $\{|E_+\rangle, |E_-\rangle\}$).

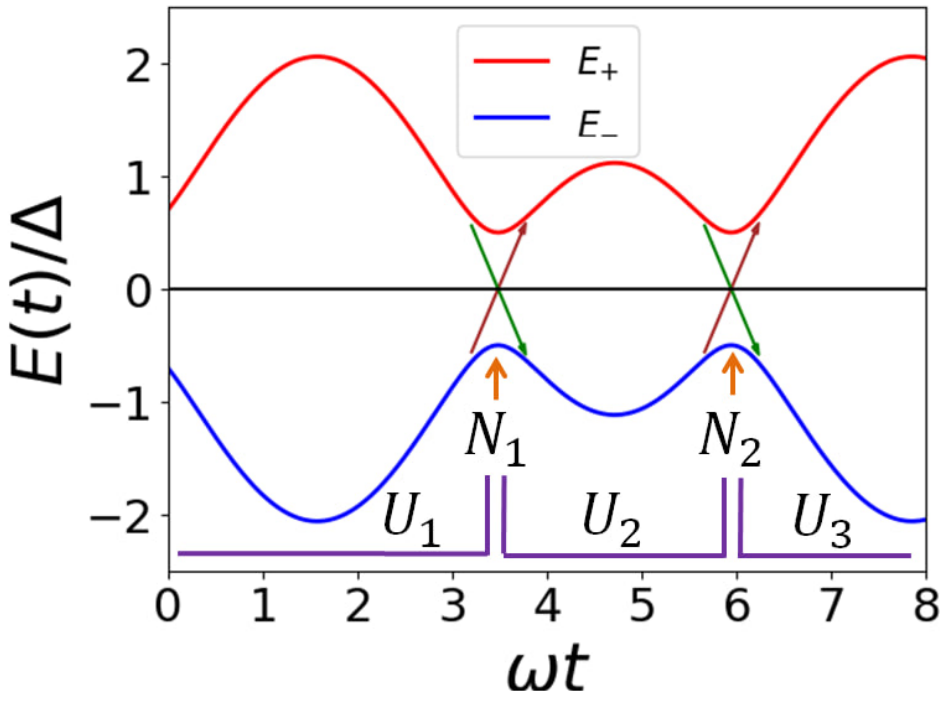

Figure 4.1 – Dynamics of system evolution. Here U_i denotes adiabatic evoluton, N_i – diabatic transition

It turns out that when the system approaches a state with a minimal value of $\varepsilon(t)$ (these points are called avoided crossings, or quasi-crossing points), a transition from the adiabatic energy level to the diabatic one can occur with a certain probability. What exactly will happen at this point depends on the rate of change $v = \dot{\varepsilon}(t)$.

At low values of v, the qubit manages to adapt. It remains at its adiabatic energy level and smoothly transitions from one physical state to another, bypassing the gap. Conversely, if v is large enough, a "jump" can occur, and the system will transition to the diabatic level, after which, as $\varepsilon(t)$ increases, it will return to the adiabatic level, but already different from the one the system was in before.

Let us try to find the probability of such a jump. To simplify the problem, we will assume that $\varepsilon_0 = 0$, and the transition time itself is sufficiently small. Then in the vicinity of the avoided crossing points $t = \pi n/\omega + t'$, $\omega|t'| \ll 1$, the following will be valid:

$$\varepsilon(\pi n/\omega + t') = \pm A \sin \omega t' \approx \pm v t', \tag{4.2}$$

where v is found from the definition as

$$v = \dot{\varepsilon}(t') \approx (A\dot{\omega}t') = A\omega. \tag{4.3}$$

Thus, in the vicinity of the avoided crossing, $\varepsilon(t)$ can be linearized using formula (4.2). Then the system's Hamiltonian $H(t)$ takes the form

$$H(t) = -\frac{\Delta}{2}\sigma_x \mp \frac{vt}{2}\sigma_z. \tag{4.4}$$

Here and below, the primes on t' will be omitted. The subsequent solution relies on the fact that under adiabatic excitation, such transitions have a semiclassical character. This is valid in cases where the change in action, given by the integral $\int E(t)dt$, is large. This reduces the problem of transitioning between adiabatic levels to a similar problem of semiclassical over-barrier reflection [36].

Suppose that at the initial moment (at $t = -\infty$), the qubit was at the lower energy level. Then the probability of transitioning to the upper level during a single passage of the avoided crossing point in this approximation is described as follows. The adiabatic energy

levels $E_{\pm}(t)$ are obtained similarly to (2.33), only for the Hamiltonian from formula (4.4):

$$E_{\pm}(t) = \pm\frac{1}{2}\sqrt{\Delta^2 + (vt)^2}. \tag{4.5}$$

These levels coincide only at two points on the complex plane. That is, solving the equation $E_{-}(t) = E_{+}(t)$, we find the required t:

$$t = \pm i\Delta/v \equiv \pm t_0. \tag{4.6}$$

Now we can use the well-known formula (see [10]), which describes the probability P_{+} that the system will be at the upper level at time $t = +\infty$:

$$P_{+} = \exp\left(-\frac{2}{\hbar}\mathrm{Im}\int_0^{t_0}[E_{+}(t) - E_{-}(t)]dt\right). \tag{4.7}$$

We calculate the integral from (4.7) using the substitution $t = \frac{\Delta}{v}z$:

$$\int_0^{t_0}\Delta E(t)dt = \frac{\Delta^2}{v}\int_0^{i}\sqrt{1+z^2}dz = \frac{\Delta^2}{2v}I\Big|_0^{i}. \tag{4.8}$$

Making simple mathematical transformations, we represent the integral I in the form

$$I = \int\sqrt{1+z^2}dz = z\sqrt{1+z^2} - I + \mathrm{asinh}(z). \tag{4.9}$$

Considering that $\mathrm{asinh}(i) = i\pi/2$, we substitute (4.9) into (4.8):

$$\frac{\Delta^2}{2v}I\Big|_0^{i} = \frac{\Delta^2}{2v}\left(z\sqrt{1+z^2} + \mathrm{asinh}(z)\right)\Big|_0^{i} = i\frac{\pi\Delta^2}{4v}, \tag{4.10}$$

Thus, we obtained the probability of such a diabatic transition P_{LZ} (it is also called the Landau-Zener probability) [10]:

$$P_{+} = P_{LZ} = \exp(-2\pi\delta), \tag{4.11}$$

where δ is the adiabaticity parameter, given by the expression

$$\delta = \frac{\Delta^2}{4\hbar v} = \frac{\Delta^2}{4\hbar A\omega}. \tag{4.12}$$

Let us analyze the obtained result. As stated earlier, at small values of v the system will evolve adiabatically (without jumps). From formula (4.12) it follows that as $v \to 0$, $\delta \to \infty$, and, as a consequence $P_{LZ} \to 0$, which matches expectations. This is called the adiabatic limit. Conversely, for large v, the parameter δ tends to 0, and $P_{LZ} \to 1$.

The numerical solution of the Schrödinger equation with the Hamiltonian (4.4) (see Fig. 4.2) also demonstrates that the probability of being at the higher energy level changes very quickly and becomes close to P_{LZ}.

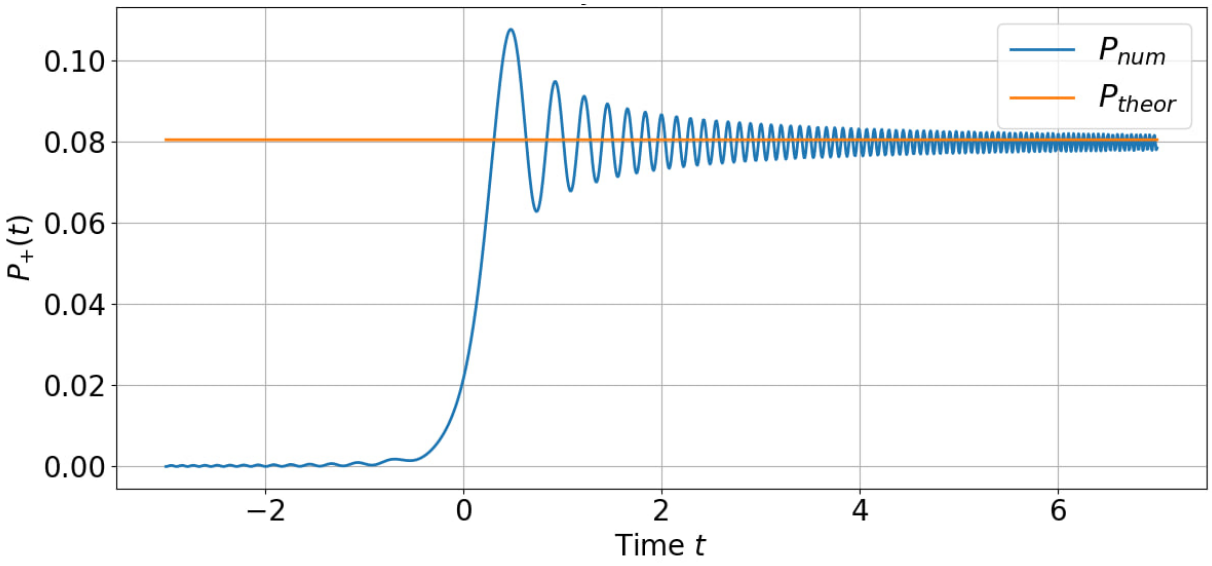

Figure 4.2 – Landau–Zener transition at the single passage

4.2 Transfer-matrix method for selecting parameters to implement quantum gates

Given the complexity of an exact analytical solution to the Schrödinger equation in the diabatic basis for Hamiltonian (4.4), it makes sense to consider the entire process of the qubit's evolution as a sequence of applying adiabatic U_i and diabatic N_i evolution operators to the state function (see Fig. 4.1). At the same time, we assume that jumps between energy

levels occur almost instantaneously. This approach is called the transfer-matrix method. Let us consider these stages separately.

4.2.1 Adiabatic evolution

Adiabatic evolution is described by the time evolution operator, which in the adiabatic basis $\{|E_+\rangle, |E_-\rangle\}$ has a simple diagonal form:

$$U(t_i, t_j) = \begin{pmatrix} e^{-i\zeta(t_i,t_j)} & 0 \\ 0 & e^{i\zeta(t_i,t_j)} \end{pmatrix} = e^{-i\zeta\sigma_z} = R_z(2\zeta), \tag{4.13}$$

where $\zeta(t_i, t_j)$ is the phase accumulated during the adiabatic evolution:

$$\zeta(t_i, t_j) = \frac{1}{2\hbar}\int_{t_i}^{t_j} \Delta E(t)dt = \frac{1}{2\hbar}\int_{t_i}^{t_j} \sqrt{\Delta^2 + \varepsilon(t)^2}dt. \tag{4.14}$$

This expression (4.13) is quite easily derived from the solution of the time-dependent Schrödinger equation.

It is easy to verify that $U(t_i, t_j)$ is, in essence, a state rotation operator around the z axis by an angle 2ζ:

$$U(t_i, t_j) = e^{-i\zeta\sigma_z} = R_z(2\zeta). \tag{4.15}$$

4.2.2 Diabatic transitions

The diabatic evolution (transition) for passing the avoided crossing point in the direction of increasing energy shift $\varepsilon(t)$ can be written in the form of a matrix

$$N = \begin{pmatrix} Re^{-i\phi_S} & -T \\ T & Re^{i\phi_S} \end{pmatrix}, \tag{4.16}$$

where $T = \sqrt{P_{LZ}}$ and $R = \sqrt{1 - P_{LZ}}$ are the transmission and reflection coefficients respectively, and ϕ_S is the Stokes phase [9], which is given by the expression

$$\phi_S = \frac{\pi}{4} + \delta(\ln\delta - 1) + \mathrm{Arg}[\Gamma(1 - i\delta)]. \tag{4.17}$$

A complete derivation of formula (4.16) is presented in [9]. Like the adiabatic evolution expression, this operator can be decomposed into a sequence of rotations around the principal axes:

$$N = R_z(\phi_S)R_y(\theta)R_z(\phi_S), \tag{4.18}$$

where the angle θ is found from the equation $\sin^2(\theta/2) = P_{LZ}$.

It is important to note the fact that the form of operator N depends on whether $\varepsilon(t)$ is increasing or decreasing at the avoided crossing point. In particular, for the reverse passage ($\varepsilon(t)$ decreases), expression (4.16) must transform into

$$N^{inv} = N^T = \begin{pmatrix} Re^{-i\phi_S} & T \\ -T & Re^{i\phi_S} \end{pmatrix}. \tag{4.19}$$

4.2.3 Methodology for selecting control parameters

From the previous subsections 4.2.1 and 4.2.2, it can be concluded that one full LZSM transition can be described by the following set of matrices:

$$U_{LZSM} = U(t_1, t_2)N_1U(0, t_1). \tag{4.20}$$

It would seem that by a proper choice of the control parameters A, Δ, ε, ω, one can create any arbitrary unitary gate of the form $U_{gate} = U_{LZSM}$. However, this is not exactly true. Expression (4.20) does not allow making transitions for which $\theta = \pi$, which follows from formula (4.11) and is manifested in the impossibility of selecting such parameters that exactly satisfy $P_{LZ} = 1$. Therefore, for the implementation of an arbitrary logic gate, it is necessary to consider at least two passages through the avoided crossing point. Thus, we obtain the matrix equation

$$U_{gate} = U(t_2, t_3)N_2^TU(t_1, t_2)N_1U(0, t_1). \tag{4.21}$$

By solving it, one can find such field parameters that would allow realizing an arbitrary gate U_{gate} with high accuracy via a double LZSM transition. However, the number of transitions for a single gate can be increased (for example, to 4), which allows increasing the accuracy of this operation's execution. More details on this are provided in [19].

SECTION 5. NUMERICAL MODELING OF QUANTUM GATES

This section presents the results of numerical modeling of the X-gate implemented by various quantum control methods (using Rabi oscillations and LZSM transitions), as well as a detailed analysis of them.

5.1 Relaxation and decoherence times

As already noted in 3.2, the dissipative influence of the environment on a quantum system can be divided into two fundamentally different physical mechanisms. These include relaxation, which has a characteristic time T_1, and dephasing, characterized by the time T_2 (see formula (3.48)). Let us briefly describe them.

Longitudinal (energy) relaxation T_1 is essentially a process of energy exchange between the qubit and the environment. For systems in thermal equilibrium at low temperatures, this process corresponds to the spontaneous transition of the system from an excited state to the ground state. During this, the qubit's energy is irreversibly released into the environment. On the Bloch sphere, the process of the system's evolution in the presence of relaxation manifests as a gradual shift of the z-component of the Bloch vector to some equilibrium value. If the environment's temperature is significantly lower than the system's temperature, this equilibrium state will correspond to the pole $|0\rangle$.

Dephasing describes the process of the qubit losing phase coherence. In this case, energy exchange is not necessary, but information about the system's state is lost. The result is the decay of the off-diagonal elements of the density matrix ρ. On the Bloch sphere, this process looks like a "blurring" of the state vector along the equator, which transitions into an explicit exponential decrease of its x- and y-components. In fact, the Bloch vector "shrinks" to the z axis.

In reality, these two parameters are not independent. Since energy relaxation also causes the destruction of phase superposition, the characteristic time of complete coherence loss can be defined as

$$\frac{1}{T_2} = \frac{1}{2T_1} + \frac{1}{T_\phi}, \tag{5.1}$$

where T_ϕ is the pure dephasing time [2].

From this equality follows a strict physical constraint on the possible system parameters: $T_2 \leq 2T_1$.

5.2 Comparison of the Rabi-based and LZSM-based X-gate with dissipation

We will consider the process of executing the X-gate (see formula (2.21)) using different control methods – the traditional resonant method via Rabi oscillations and the fast non-resonant method using LZSM transitions. Modeling of the open system's evolution process was performed using methods of numerical integration of the modified Bloch equations (3.53).

We choose $|0\rangle$ as the initial state. The magnetic field is sinusoidal with tunneling amplitude and offset equal to $\Delta = 1$ and $\varepsilon_0 = 0$, respectively. For Rabi oscillations, the frequency is found automatically from formula (3.1) and is $\omega_L = 1$ (we work in a system of units where $\hbar = 1$). We choose the amplitude equal to $A_R = 0.1$ (weak field case). For LZSM transitions, these two parameters are found using the method described in 4.2.3. This gives us a number of options, among which we choose the pair $A_L = 4.6995$ and $\omega_L = 0.4822$. Here and below, all specified quantities are dimensionless (normalized to Δ and $\hbar$ as needed).

Let us start by comparing the Bloch vector evolution process for both quantum control methods. The obtained result demonstrates the fundamental difference in the performance speed of both approaches (see Fig. 5.1).

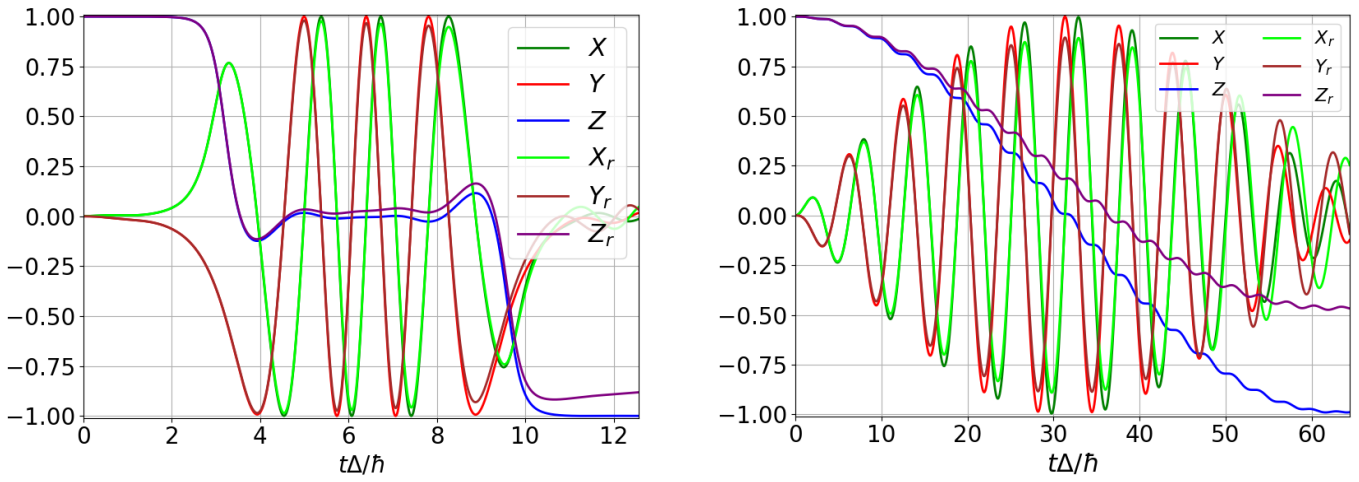

Figure 5.1 – Dynamics in ideal (no relaxation; the components of the Bloch vector X, Y, Z) and real (with relaxation; the components of the Bloch vector X_r, Y_r, Z_r) systems with $\frac{\Delta}{\hbar}T_{1,2} = 100$ for LZSM-based (left panel) and Rabi-based (right panel) X-gate

As we can see, the duration of the Rabi transition is $t \approx 63$, which in this case is already comparable in order of magnitude to the decoherence T_2 and relaxation T_1 times. This makes them inapplicable under the condition of strong interaction of the qubit with the environment. Overall, the Rabi oscillations-based gate not only takes several times longer (which is already a poor result in itself) but also expectedly yields a significantly larger error. Visually, this manifests in the differences between the Z and Z_r components of the Bloch vector. However, we note that such short characteristic times of dissipative processes were chosen for demonstrative purposes. Although, even with their increase, the Rabi-based method has lower accuracy, which will be shown below.

Nevertheless, it is not explicitly clear from Fig. 5.1 whether this error is a consequence of dissipative processes or simply an inaccuracy in selecting the control parameters. Therefore, we perform a 3D modeling of the state point's movement on the Bloch sphere for the LZSM (see Fig. 5.2) and Rabi (see Fig. 5.3) X-gate.

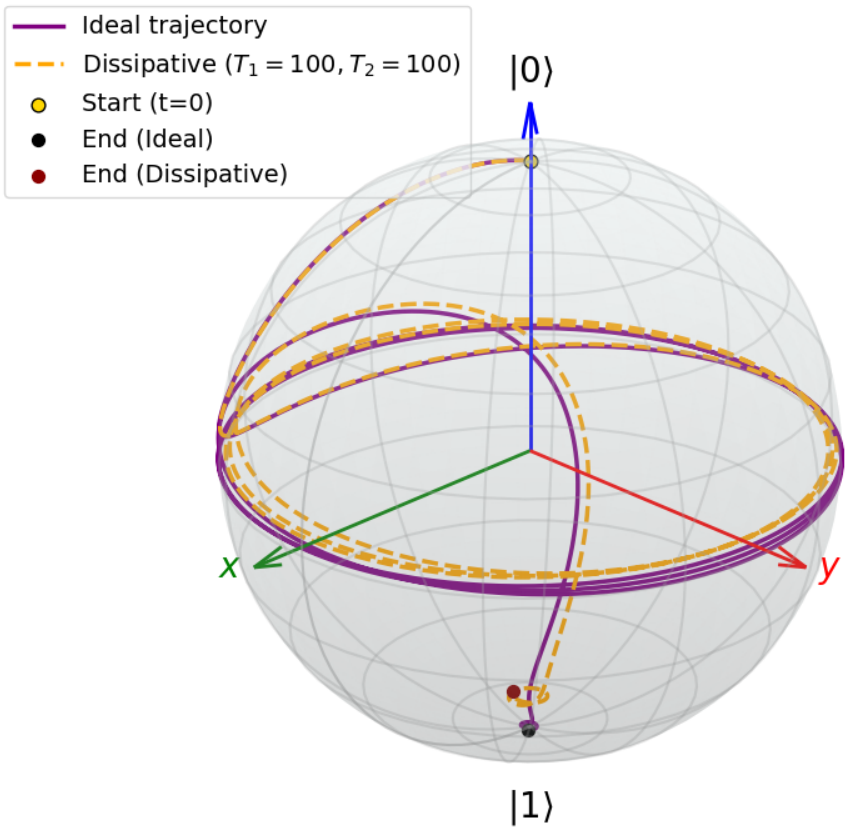

Figure 5.2 – Evolution of the state on the Bloch sphere for the LZSM-based X-gate

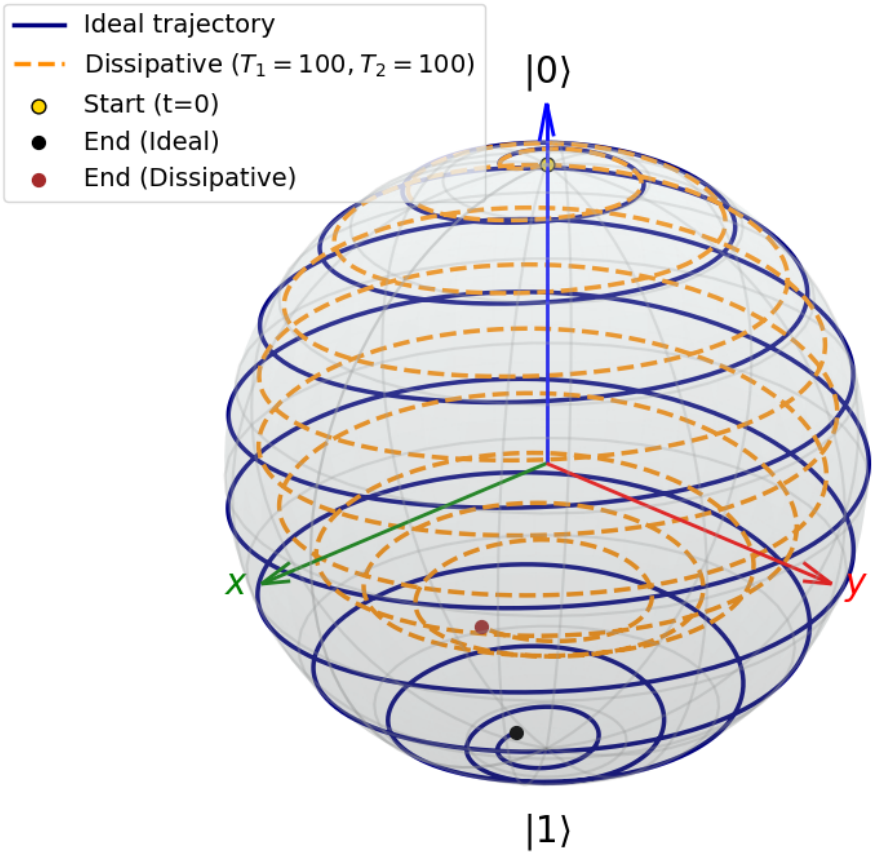

Figure 5.3 – Evolution of the state on the Bloch sphere for the Rabi-based X-gate

The results not only confirm the lower error of the LZSM transition-based gate but also show that the state vector is inside the Bloch sphere, which was described in 5.1 and is a sign of the system transitioning into a mixed state. It is also interesting that from Fig. 5.3 one can see a not absolutely exact convergence with the expected result even for an ”ideal” Rabi gate. However, this error is no longer related to dissipation, but to the Rabi approach itself. This is a consequence of using the rotating-wave approximation, which over time manifests in the accumulation of intrinsic (hardware) errors.

Finally, let us now conduct a more quantitative study. We fix one of the characteristic dissipation times and will calculate the error of the probabilities of the system being in the expected state $|1\rangle$ after applying the X-gate. Fig. 5.4 demonstrates the dependence of this error on the relaxation time T_1, and Fig. 5.5 – on the decoherence time T_2. Note that for the case of dependence on T_1, the decoherence time cannot be assumed infinite, because relaxation itself leads to phase loss. Mathematically, this is a consequence of expression (5.1). It can also be noticed that in Fig. 5.4, at small values of T_1, the errors for the Rabi-

based gate begin to reach a stationary value. This is a direct consequence of the fact that the duration of one such operation coincides in order of magnitude with the relaxation time.

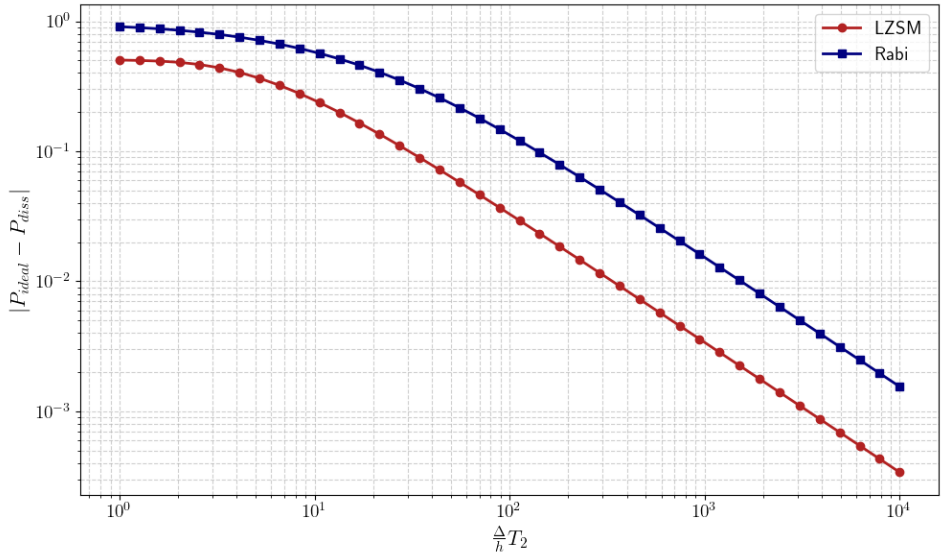

Figure 5.4 – Dependence of the probability error on T_1 at $T_2 = 10$ for both methods

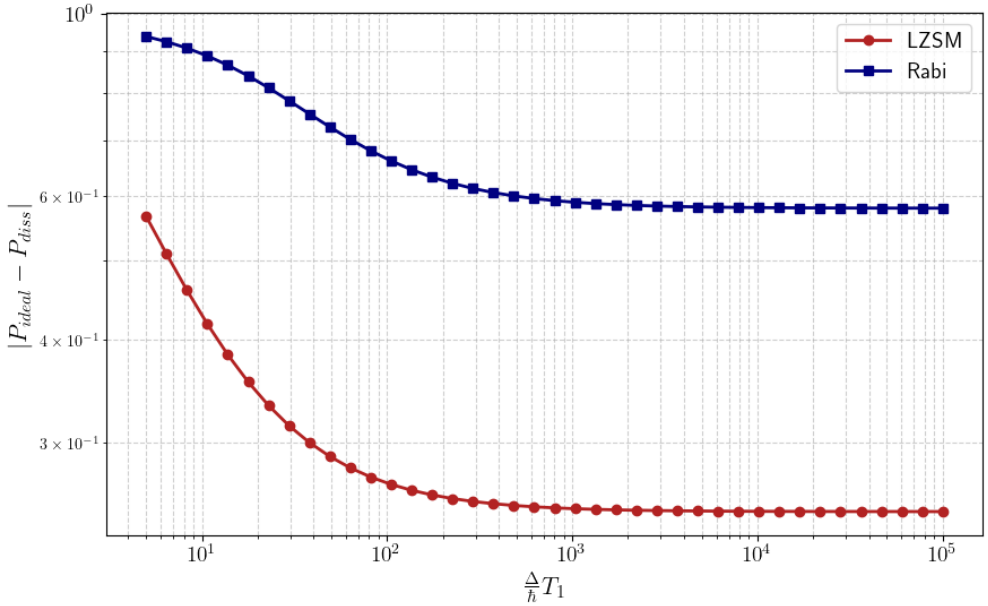

Figure 5.5 – Dependence of the probability error on T_2 at $T_1 = \infty$ for both methods

The presented modeling results confirm the higher accuracy of using LZSM transitions for qubit state control compared to the traditional resonant method.

5.3 Fidelity distribution on the Bloch sphere for the LZSM- and Rabi-based X-gates

As noted in 5.1, there is always some equilibrium state of the environment that the system's state approaches (except for situations with powerful perturbations in the environment). As a result, a quite logical thought arises that the fidelity F of performing computations using a quantum gate U must depend on what state the qubit should end up in after applying all operations. Consequently, the accuracy of the obtained result also depends on the initial qubit state ρ_{in}. Let us now analyze how this affects computation errors.

By definition [37], the computation fidelity is determined using the formula

$$F(\rho, \rho_{in}) = \left(\mathrm{Tr} \sqrt{\sqrt{\rho} U \rho_{in} U^{\dagger} \sqrt{\rho}} \right)^2 . \tag{5.2}$$

We select a set of initial states uniformly distributed over the Bloch sphere, and calculate the accuracy of applying the X-gate for them. The control parameters for both methods remain the same as during the modeling in 5.2, and the characteristic times of dissipative processes are $T_1 = T_2 = 100$. Considering that the obtained distributions are three-dimensional and cannot be fully demonstrated in a 2D format, Fig. 5.6 and Fig. 5.7 show 3 of their projections in the yz, xz, and xy planes, respectively.

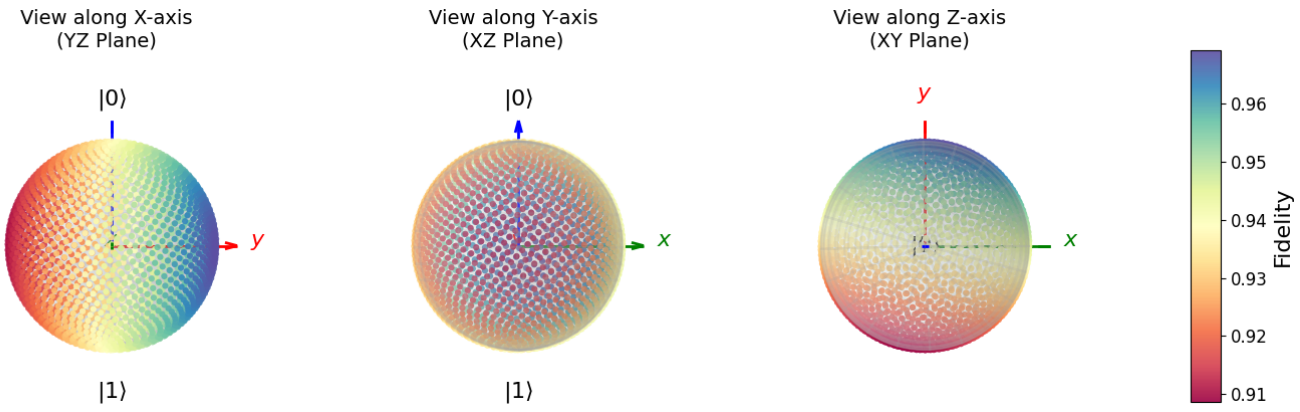

Figure 5.6 – Fidelity distribution over $N = 2000$ initial states for the LZSM-based X-gate

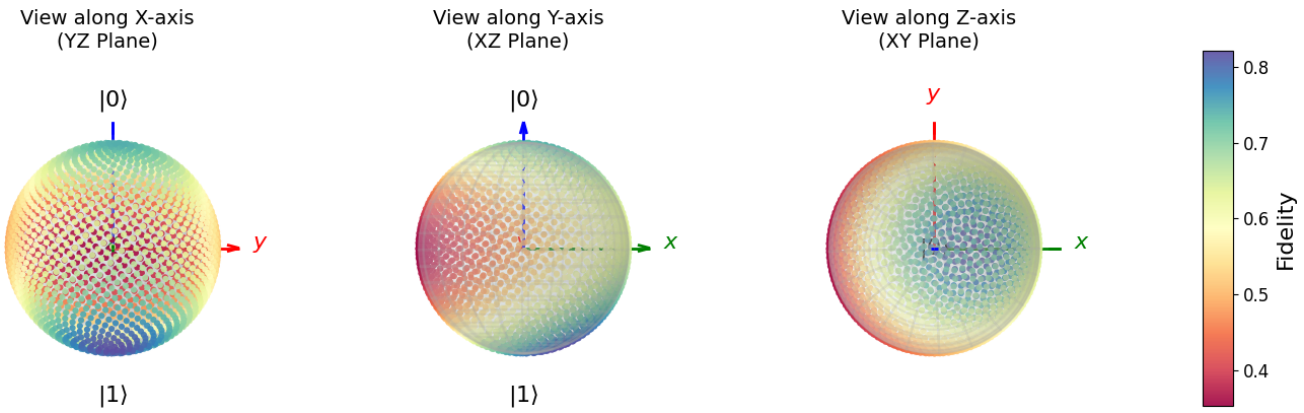

Figure 5.7 – Fidelity distribution over $N = 2000$ initial states for the Rabi-based X-gate

Let us analyze the obtained results. The modeling shows that the global fidelity level for the LZSM transition-based gate lies within the range of $0.910 - 0.965$, while for Rabi oscillations it drops to critical values of $0.40 - 0.82$. This is a direct consequence of the difference in the execution speed of the respective operation, which was described in 5.2.

The Rabi gate is characterized by asymmetry in the equatorial plane. Under the condition of an ideal execution of the Rotating-Wave Approximation (RWA), Rabi trajectories should be symmetrical. However, since we used the full Hamiltonian in the modeling, the counter-rotating terms create a shift in the precession axis, bending it. As a result, trajectories starting from opposite states on the equator (e.g., $\frac{|0\rangle+|1\rangle}{\sqrt{2}}$ and $\frac{|0\rangle-|1\rangle}{\sqrt{2}}$) pass through different latitudes on the Bloch sphere and experience different averaged effects of relaxation processes. This leads to the appearance of large zones with low fidelity near the equator on the Bloch sphere (see Fig. 5.7). In addition, the modeling demonstrates a clear vertical asymmetry – the lower hemisphere (near $|1\rangle$) has higher fidelity than the upper one (near $|0\rangle$). The reason for this lies in the direction of action of energy relaxation, which always tries to bring the system to thermodynamic equilibrium with the environment — the $|0\rangle$ state.

For the LZSM gate, such a contrasting difference in fidelity for the upper and lower hemispheres is not observed, which is a consequence of their shorter duration and, as a result, a smaller impact of relaxation. However, dephasing acts most intensely where the x and y components of the Bloch vector are maximal (i.e., near the equator). Because of this, trajectories that minimally lie in the equatorial plane maintain higher accuracy.

Conversely, vectors that linger in the vicinity of the equator due to the specific geometry of the LZSM transition accumulate a significantly larger phase error.

The obtained results are a demonstration of how spatially complex trajectories end up under different types of dissipative influences along their path.

CONCLUSIONS

In this master's thesis, a comprehensive theoretical and numerical study of qubit evolution in a dissipative environment during the execution of basic logic operations was conducted. By numerically integrating the modified Bloch equations, the following main results were obtained:

1. Fundamental advantage of non-adiabatic control: It has been quantitatively proven that logic gates based on non-adiabatic Landau-Zener-Stückelberg-Majorana (LZSM) transitions demonstrate significantly higher robustness to dissipation compared to classical Rabi pulses. Under identical environmental parameters ($T_1 = T_2 = 100$), the overall fidelity of the X-gate execution using the LZSM method ranges from 0.910 to 0.965, while for the Rabi method, this indicator drops to 0.40–0.82. This is due to the fact that the ultrafast non-adiabatic resonance crossing minimizes the interaction time of the qubit with the thermostat.

2. Limiting effect of dephasing: The study of parametric dependencies showed that with an arbitrary increase in the energy relaxation time, the total error of the quantum gate reaches an asymptotic plateau, the level of which is strictly limited by the phase coherence time. At the same time, the long duration of the Rabi gate makes it fundamentally unviable in systems with strong dephasing, since the destruction of coherence occurs faster than the completion of the logic operation itself.

3. Topological anomalies of resonant control: The construction of 3D fidelity distributions on the Bloch sphere revealed critical shortcomings of the Rabi method beyond idealized models. The rejection of the rotating-wave approximation (RWA) allowed capturing the influence of counter-rotating terms, which generate the Bloch-Siegert shift. The consequence of this shift is the tilt of the effective precession axis, which leads to a severe asymmetry of trajectories in the equatorial plane and uneven error accumulation for orthogonal initial states.

4. Chirality of LZSM transitions: It was established that for LZSM transitions, the regions of fidelity degradation form complex spiral-like structures. This effect is explained by the chirality of the control field: the harmonic sweeping of the energy detuning creates a spatial asymmetry, causing the state vectors to describe different geometric curves. Trajectories that linger near the equatorial plane experience an exponentially greater impact of transverse relaxation.

5. Application prospects: The obtained results and the developed software tools have direct practical significance for control optimization in modern quantum processors (e.g., based on superconducting transmons). The use of fast non-resonant methods is an effective tool for increasing computational fidelity in the NISQ (Noisy Intermediate-Scale Quantum) era, while hardware error correction remains technologically inaccessible.

LIST OF REFERENCES

1. T. D. Ladd *et al.*, Quantum computers, Nature **464**, 45 (2010).

2. P. Krantz, M. Kjaergaard, F. Yan, T. P. Orlando, S. Gustavsson, and W. D. Oliver, A quantum engineer's guide to superconducting qubits, Appl. Phys. Rev. **6**, 021318 (2019).

3. T. Otsuka *et al.*, Single-electron spin resonance in a quadruple quantum dot, Sci. Rep. **6**, 31820 (2016).

4. W. Gerlach and O. Stern, Der experimentelle Nachweis der Richtungsquantelung im Magnetfeld, Z. Phys. **9**, 349 (1922).

5. I. I. Rabi, Space quantization in a gyrating magnetic field, Phys. Rev. **51**, 652 (1937).

6. A. Abragam, *The Principles of Nuclear Magnetism* (Oxford University Press, New York, 1961).

7. I. I. Rabi *et al.*, A new method of measuring nuclear magnetic moment, Phys. Rev. **53**, 318 (1938).

8. S. N. Shevchenko, S. Ashhab, and F. Nori, Landau-Zener-Stückelberg interferometry, Phys. Rep. **492**, 1 (2010).

9. O. V. Ivakhnenko, S. N. Shevchenko, and F. Nori, Nonadiabatic Landau-Zener-Stückelberg-Majorana transitions, dynamics, and interference, Phys. Rep. **995**, 1 (2023).

10. L. D. Landau, Zur Theorie der Energieubertragung II, Phys. Z. Sowjetunion **2**, 46 (1932).

11. C. Zener, Non-adiabatic crossing of energy levels, Proc. R. Soc. Lond. A **137**, 696 (1932).

12. E. C. G. Stückelberg, Theorie der unelastischen Stösse zwischen Atomen, Helv. Phys. Acta **5**, 369 (1932).

13. E. Majorana, Atomi orientati in campo magnetico variabile, Nuovo Cimento **9**, 43 (1932).

14. W. D. Oliver *et al.*, Mach-Zehnder interferometry in a strongly driven superconducting qubit, Science **310**, 1653 (2005).

15. S. Ashhab, J. R. Johansson, A. M. Zagoskin, and F. Nori, Two level systems driven by large-amplitude fields, Phys. Rev. A **75**, 063414 (2007).

16. D. L. Campbell, Y.-P. Shim, B. Kannan, R. Winik, D. K. Kim, A. Melville, B. M. Niedzielski, J. L. Yoder, C. Tahan, S. Gustavsson, and W. D. Oliver, Universal nonadiabatic control of small-gap superconducting qubits, Phys. Rev. X **10**, 041051 (2020).

17. C. Hicke, L. F. Santos, and M. I. Dykman, Fault-tolerant Landau-Zener quantum gates, Phys. Rev. A **73**, 012342 (2006).

18. H. Zhang *et al.*, Universal fast-flux control of a coherent, low-frequency qubit, Phys. Rev. X **11**, 011010 (2021).

19. A. I. Ryzhov, O. V. Ivakhnenko, S. N. Shevchenko, M. F. Gonzalez-Zalba, and Franco Nori, Alternative fast quantum logic gates using nonadiabatic Landau-Zener-Stückelberg-Majorana transitions, Phys. Rev. Res. **6**, 033340 (2024).

20. N. V. Vitanov and K. A. Suominen, Nonlinear level-crossing models, Phys. Rev. A **59**, 4580 (1999).

21. M. Kuzmanovič, I. Björkman, J. J. McCord, S. Dogra, and G. S. Paraoanu, High-fidelity robust qubit control by phase-modulated pulses, Phys. Rev. Res. **6**, 013188 (2024).

22. T. Araki, F. Nori, and C. Gneiting, Robust quantum control with disorder-dressed evolution, Phys. Rev. A **107**, 032609 (2023).

23. N. Khaneja *et al.*, Optimal control of coupled spin dynamics: design of NMR pulse sequences by gradient ascent algorithms, J. Magn. Reson. **172**, 296 (2005).

24. A. G. Fowler *et al.*, Surface codes: Towards practical large-scale quantum computation, Phys. Rev. A **86**, 032324 (2012).

25. P. A. M. Dirac, *The Principles of Quantum Mechanics* (Oxford University Press, Oxford, 1981).

26. M. A. Nielsen and I. L. Chuang, *Quantum Computation and Quantum Information* (Cambridge University Press, Cambridge, 2010).

27. M. Born and E. Wolf, *Principles of Optics* (Cambridge University Press, Cambridge, 1999).

28. P. Kaye, R. Laflamme, and M. Mosca, *An Introduction to Quantum Computing* (Oxford University Press, New York, 2006).

29. J. von Neumann, *Mathematical Foundations of Quantum Mechanics* (Princeton University Press, Princeton, 1955).

30. H.-P. Breuer and F. Petruccione, *The Theory of Open Quantum Systems* (Oxford University Press, Oxford, 2002).

31. L. D. Landau and E. M. Lifshitz, *Quantum Mechanics: Non-Relativistic Theory* (Pergamon Press, Oxford, 1977).

32. D. J. Griffiths and D. F. Schroeter, *Introduction to Quantum Mechanics* (Cambridge University Press, Cambridge, 2018).

33. M. Abramowitz and I. A. Stegun, *Handbook of Mathematical Functions* (National Bureau of Standards, Washington, DC, 1964).

34. L. Allen and J. H. Eberly, *Optical Resonance and Two-Level Atoms* (Dover Publications, New York, 1987).

35. L. D. Landau and E. M. Lifshitz, *Statistical Physics, Part 1*, 3rd ed. (Butterworth-Heinemann, Oxford, 1980).

36. L. D. Landau and E. M. Lifshitz, *Quantum Mechanics: Non-Relativistic Theory*, 3rd ed. (Pergamon, Oxford, 1977).

37. R. Jozsa, Fidelity for mixed quantum states, J. Mod. Opt. **41**, 2315 (1994).